



University of  
Massachusetts  
Amherst

## Detection of Benzoyl Peroxide in Flour Using Raman Spectroscopy

Item Type	Thesis (Open Access)
Authors	Ho, Yu
DOI	<a href="https://doi.org/10.7275/26842220.0">10.7275/26842220.0</a>
Rights	Attribution 4.0 International
Download date	2026-03-14 13:25:01
Item License	<a href="http://creativecommons.org/licenses/by/4.0/">http://creativecommons.org/licenses/by/4.0/</a>
Link to Item	<a href="https://hdl.handle.net/20.500.14394/32830">https://hdl.handle.net/20.500.14394/32830</a>

## Detection of Benzoyl Peroxide in Flour Using Raman Spectroscopy

Yu Ho

Follow this and additional works at: [https://scholarworks.umass.edu/masters\\_theses\\_2](https://scholarworks.umass.edu/masters_theses_2)



Part of the [Food Science Commons](#)

---

**Detection of Benzoyl Peroxide in Flour using Raman Spectroscopy**

A Dissertation Presented

by

Yu Ho

Submitted to the Graduate School of the  
University of Massachusetts Amherst in partial fulfillment  
of the requirements for the degree of

Master of Science

February 2022

Department of Food Science

© Copyright by Yu Ho 2022

All Rights Reserved

# Detection of Benzoyl Peroxide in Flour using Raman Spectroscopy

A Dissertation Presented

by

Yu Ho

Approved as to style and content by:

---

Lili He, Chair

---

Jiakai Lu, Member

---

Lutz Grossmann, Member

---

Lynne A. McLandsborough, Director  
Department of Food Science

## **ACKNOWLEDGMENTS**

I would like to thank my advisor, Dr. Lili He for her. Patience and constant motivation on my master research and life. Her suggestions in study and opinions for research always motivated me to move forward in the food science field, even during the pandemic. I am grateful to be her student.

I would also like to thank my committee members, Dr. Jiakai Lu and Dr. Lutz Grossmann for their time and recommendations. Finally, a huge thanks to all my lab mates for their feedback and cooperation.

**ABSTRACT**  
**DETECTION OF BENZOYL PEROXIDE IN FLOUR USING RAMAN**  
**SPECTROSCOPY**

FEBRUARY 2022

YU HO, B.A., UNIVERSITY OF MASSACHUSETTS AMHERST

M.A., UNIVERSITY OF MASSACHUSETTS AMHERST

Directed by: Dr. Lili He

Benzoyl peroxide (BPO) is a common bleaching agent used in wheat flour. Due to its ability to damage existing nutrients in food and potential adverse effect to health, BPO have been strictly banned as a food additive in several countries and regions, such as China and Europe. However, the United States specifies that BPO is generally recognized as safe (GRAS). So, the WHO/FAO created a Codex Alimentarius Commission (CAC) to regulate the international BPO usage standard. According to the CAC, it is restricted at 75 mg/kg or parts per million (ppm). BPO is very unstable and easily converts to benzoic acid (BA), which places the analytical challenge for accurate BPO quantification. The objective of this study is to develop a reliable method for BPO quantification in flour. Raman spectroscopy was first explored to detect BPO and BA on an aluminum foil slide. The result showed BPO and BA produced distinct Raman peaks that can be discriminated against. However, the sensitivity was not satisfactory to reach the regulation limit. To improve sensitivity, surface-enhanced Raman spectroscopy (SERS) was applied using silver nanoparticles as the substrate. Although the signals did enhance significantly using SERS, the characteristic peaks of BPO disappeared as BPO converted to BA during the sample preparation. We then went back to Raman spectroscopy but focused on optimizing the sample preparation to enhance the signal intensity. Using a hydrophobic

surface (i.e., parafilm) which can hold the droplet and minimize the spread, the Raman signal was enhanced significantly after repeating multiple droplets on the same surface. A standard curve was created for BPO from 25 ppm to 250 ppm and for BA from 250 ppm to 1000 ppm, respectively. To detect BPO in wheat flour, we applied a more advanced Raman imaging instrument and focused on the analysis of Raman maps instead of spectra for the analysis of effect flour matrix to BPO extraction and detection. We firstly tried an *in situ* method, which scanned the pellet of flour spiked with different amounts of BPO without extraction. However, we could not detect BPO at 0.1% or lower in flour samples. We then tried an extraction method using acetonitrile as the solvent, which showed a lower detection limit compared to the *in situ* method. However, this extraction method yielded inconsistent results for BPO that is under 0.05% in flour. The extraction method developed was further improved with an evaporating step and a C18 solid phase extraction (SPE) spin column. This improved the extraction efficacy and provided a roughly 60% recovery percentage for detecting BPO in wheat flour without decomposing into BA. In conclusion, we developed a simple sample preparation protocol coupled with Raman spectroscopy to quantify BPO in flour without converting to BA, which would meet the regulation requirement. This method also shortened the experiment time including both sample preparation and detection time compared to current methods.

# TABLE OF CONTENTS

	Page
Acknowledgments.....	vii
Abstract.....	vii
List of tables.....	vii
List of figures.....	vii
Chapter 1 Introduction.....	1
1.1 Benzoyl peroxide, Benzoic acid, and their application.....	1
1.2 Regulation of BPO and BA in foods.....	3
1.3 Current analytical method of BPO and BA detection in Foods.....	4
1.3.1 Detection of BPO.....	4
1.3.2 Detection of BA.....	6
1.4 Raman Spectroscopy and Surface Enhanced Raman Spectroscopy.....	7
1.5 Goals and objectives.....	11
Chapter 2 Development of a droplet method for Raman spectroscopy to quantify Benzoyl peroxide and Benzoic acid.....	12
2.1 Introduction.....	12
2.2 Material and sample preparation.....	14
2.2.1 Materials.....	14
2.2.2 Substrate and sample preparation.....	14
2.2.2.1 Normal Raman.....	14
2.2.2.2 SERS.....	14
2.2.2.3 SERS +antioxidant.....	15
2.2.2.4 Normal Raman (parafilm surface +running method) .....	15
2.2.3 Raman Analysis.....	15
2.3 Result and discussion.....	17
2.3.1 Normal Raman (aluminum surface) .....	17
2.3.2 SERS.....	18
2.3.3 SERS +antioxidant.....	20
2.3.4 Normal Raman (parafilm surface +running method) .....	22
2.4 Conclusion.....	31
Chapter 3 Evaluate the flour matrix effect on BPO detection in flour samples.....	33
3.1 Introduction.....	33
3.2 Material and methods.....	34
3.2.1 Materials.....	34
3.2.2 Substrate and sample preparation.....	35
3.2.2.1 <i>In situ</i> method.....	35
3.2.2.1 Extraction method.....	35
3.2.3 Raman and image analysis.....	36
3.3 Result and discussion.....	38
3.3.1 <i>In situ</i> method.....	38
3.3.2 Extraction method.....	39
3.4 Conclusion.....	44
Reference.....	46

## LIST OF TABLES

Table	Page
1. Percentage of area showing BPO signal in chosen mapping from image analysis.....	38
2. Percentage of area showing BPO signal in chosen mapping by extraction method.....	39

## LIST OF FIGURES

Figure	Page
1. Benzoyl peroxide molecular structure.....	2
2. Benzoic acid molecular structure.....	2
3. Decomposition mechanisms of BPO in flour.....	3
4. Decomposition mechanism of BPO.....	13
5. Possible reaction of BPO for spectrophotometry.....	13
6. Demonstration of BPO Raman analysis. Peak at $1780\text{ cm}^{-1}$ is used to create standard curves.....	16
7. Demonstration of BA Raman analysis. Peak at $800\text{ cm}^{-1}$ is used to create standard curves.....	16
8. Average Raman spectra for 1000 ppm of BA and BPO.....	17
9. average Raman spectra of AgNPs, 100 ppm of BPO with AgNPs, and 100 ppm of BA with AgNPs.....	18
10. PCA result for BPO and BA with SERS. 70% of data were used for model establishment, and 30% of remaining as validation. BPO accuracy is 85%. BA accuracy is 90%.....	19
11. Average Raman spectra of AuNPs, 100 ppm of BPO with AuNPs, and 100 ppm of BA with AuNPs .....	20
12. SERS Raman spectra of AgNPs, 100 ppm of BHT, BPO+BHT, and BA+BHT.....	21
13. Four batches of SERS intensity at $1000\text{ cm}^{-1}$ produced from 100 ppm of BPO and BA with or without BHT. Error bars represent the standard deviation of the average signal intensity at $1000\text{ cm}^{-1}$ .....	21
14. (A) BPO droplet on aluminum plate. Droplet for 100ppm or lower barely observable (B) BPO droplet on parafilm surface. Aggregate substrate, easy to observe.....	23
15. Standard curve of BPO concentration produced from the average Raman intensity at	

1780  $\text{cm}^{-1}$ . Error bars represent the standard deviation of average signal intensity at 1780  $\text{cm}^{-1}$ . (A)(B)(C) represent three different batches of stock BPO tested. (A1)(B1)(C1) represent Raman images of average 25, 50, 100, and 250 ppm of BPO corresponding to (A)(B)(C).....24

16. Standard curve of BA concentration produced from the average Raman intensity at 800  $\text{cm}^{-1}$ . Error bars represent the standard deviation of average signal intensity at 800  $\text{cm}^{-1}$ . (D)(E) represent two different stocks of BA were tested. (D1)(E1) represent Raman images of average 250, 500, and 1000 ppm of BA corresponding to (D)(E) .28

17. Demonstrations of BPO Raman analysis. Peaks at 1780  $\text{cm}^{-1}$  are used to process image analysis and acquire BPO's area percentage.....37

18. Mapping images of BPO flour detected by Thermo Scientific DXRxi Spectro-microscope. A: 0.05% BPO flour. B: 0.01% BPO flour.....39

19. Three replicates mapping images for 0.05% BPO flour detect by DXRxi Spectro-microscope.....40

20. Three replicates mapping images for 0.01% BPO flour detect by DXRxi Spectro-microscope.....41

21. Two replicate mapping images for 75 ppm spiking BPO samples detect by DXRxi Spectro-microscope.....41

22. Two replicate mapping images for 0.1% BPO originally in flour. A provides 28.96% area of BPO presenting, and B provides 22.73% area of BPO presenting according to image analysis (C) represents the average spectrum (A) and (B).....43

23. Two replicate mapping images for 0.1% spiking BPO procedure. A shows 46.60% area of BPO presenting, and B shows 35.21% area of BPO presenting according to image analysis (C) represents the average spectrum of (A) and (B).....44

# CHAPTER 1

## Introduction

### 1.1 Benzoyl peroxide, benzoic acid, and their application

Benzoyl peroxide (BPO) (Figure 1) is a chemical compound used as a food additive or for medical purposes. When added into flour, BPO acts as a bleaching agent. It oxidizes carotenoids, such as lutein, in flour to bleach the yellow color. In medications, BPO is widely used to treat acne either alone or with other treatments. BPO appears as odorless white powder, and it is water-insoluble. BPO is relatively stable at room temperature, but it can cause combustion or explosion through impact or friction. Thus, BPO should be handled with caution. Huang (1) tested the thermal stability of BPO and found that the decomposition of BPO in a sealed container increased the risk of thermal explosion. Tan (2) found out that as pressure increased, the decomposition temperature (from initial decomposition to decomposition completion) of BPO increased slightly. In addition, BPO's self-accelerating decomposition temperature can be reduced by increasing packaging quality. Furthermore, BPO has the potential to cause cancer. Although BPO does not count as a carcinogen, it promotes cell growth when applied to an initiated tumor. (3) BPO, after entering the human body, requires the liver to neutralize it, and is therefore bad for those with a weak liver as it may cause chronic intoxication upon a long-term consumption of bleached flour products. Being a strong oxidant, BPO destroys nutrient content in flour by oxidizing beta carotene. This affects vitamin A content and causes the loss of vitamin E and K (6), and it may influence vitamin B1 and B2 as well.

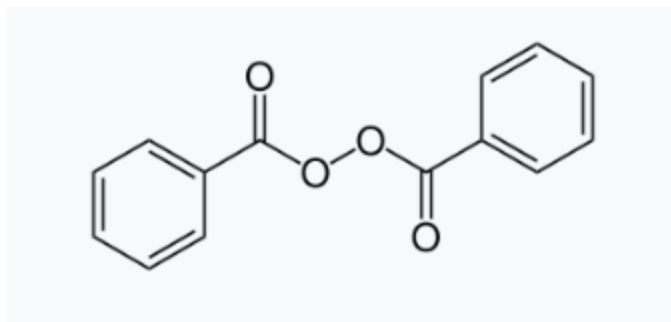


Figure 1. Benzoyl peroxide molecular structure

Benzoic acid (BA) (figure 2) is a preservative that can inhibit the growth of yeast, molds, and some bacteria. (4) The efficacy of BA is dependent on the target food's pH, and BA is usually used as a preservative in acidic food such as soft drinks, fruit juice, or other acidified products. BA appears as a white crystalline solid, and is slightly water-soluble. BA can also be used for the treatment of fungal skin disease, such as tinea or ringworm. Additionally, BA is a common precursor to plasticizers.

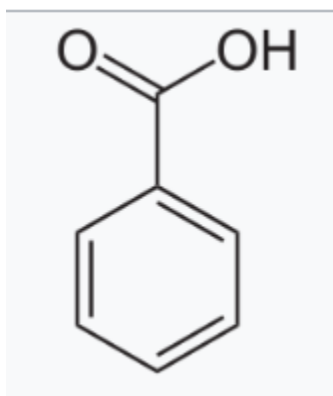


Figure 2. Benzoic acid molecular structure.

We will mainly focus on BPO and BA's function in foods. When adding BPO as a bleaching agent in flour, it reacts with oxidizable substances, such as carotenoid and then converts to BA, which in most cases are not harmful. Although BPO is almost always

converted to BA (Figure 3), it can be potentially harmful in our digestive system. If some BPO does not convert to BA, it may interfere with how the human body metabolizes linoleic and linolenic acids. (5)

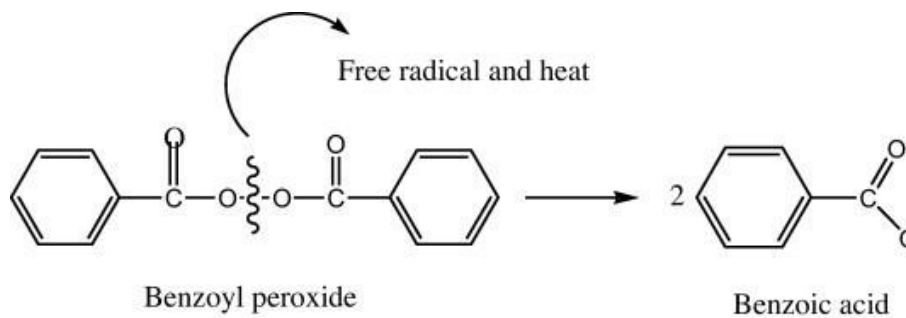


Figure 3. decomposition mechanisms of BPO in flour.

## 1.2 Regulation of BPO and BA in foods

BPO is a strong oxidant and is commonly used as a bleaching agent in flour to improve its appearance during factory processing. BPO will eventually convert to BA after oxidation due to its high instability. In the United States, the FDA has specified that BPO is GRAS according to the code of federal regulation. The WHO, however, suggests a daily dosage of only 40 mg/kg. (6) BPO is strictly banned as a bleaching agent in following countries: the European Union (due to BPO containing selenium and lead), Canada, United Kingdom, and China. In 2009, the Codex Alimentarius Commission determined that the amount of BPO allowed in wheat flour cannot be greater than 75 mg/kg or parts per million (ppm). (5)

On the other hand, BA can be added as a food preservative into foods-- soft drink being a common example. The BA we detected from flour is a main final product from

degradation of BPO. BA can also be legally used in flour products according to the standard regulation. The amount is not greater than 0.1 percent (or 1000 ppm) in flour. Unlike BPO, BA has the same regulations among countries. WHO's International Programme on Chemical Safety (IPCS) provided a provisional tolerable intake for humans which was 5 mg/kg body weight per day. (7)

## **1.3 Current analytical methods of BPO and BA detection in Foods**

### **1.3.1 Detection of BPO**

High-Performance Liquid Chromatography (HPLC) is one of the most methods to determine the amount of BPO present in wheat flour. For HPLC, establishing a standard curve and sample preparations are important steps. For BPO calibration graph, BPO was dissolved in diethyl ether and diluted with the same solvent to make the work solution. Then, ppm of BPO in the working solution were correlated with the ppm of the BPO in flour according to the extraction procedure to make the standard curve like area vs ppm of BPO in flour. (8) For sample preparation, BPO must be extracted from the bleached flour first and then converted to BA for later analysis. The procedure for extraction of BPO was developed in a flask containing 100 ml of diethyl ether and 50 g of bleached flour. Then, this mixture was shaken by a magnetic stirrer for 10 minutes and was left in repose for 15 minutes. The upper layer of the solution with extracted products from the reaction was removed with a pipet and then stored in a tube holding ice until later HPLC injection. At this step, BPO was converted to BA completely. The mobile phase used to determine BA was methanol/water (80:20). The analysis was carried out by a UV-vis detector. The BA's concentration collected from the HPLC injection method was then

calculated to acquire the BPO's concentration. This analytical method has limitations. If the samples contain both BPO and BA, the BA concentration collected can be either BPO conversion or BA itself.

The spectrophotometric method is one of many ways to determine BPO amount in flour. The concept for this method is based on the BPO reacting with ABTS to obtain a blue-green colored product. (9) For sample preparation of BPO assay, bleached flour was transferred into a centrifuge tube with ethanol. The sample then underwent sonification for 5 minutes and was completed by vortexing the solution for 5 minutes. Lastly, the supernatant was extracted after being centrifuged. To analyze the BPO, the procedures were started by adding an extraction supernatant with a tiny amount of ABTS and a large amount of ethanol and the solution reacted for 1 minute. The mixture changed color from light-green to green. The content of BPO in the sample was then calculated using the linear regression equation of standard curve. (9) Due to BPO's instability, it converted to BA after the addition of ABTS. (9) Same as HPLC, the spectrophotometric method cannot quantify for BPO and BA precisely if the sample contained both BPO and BA.

The fluorescent analytical method is another popular way for BPO detection. The concept for Fluorescent analysis is mixing BPO with fluorescent conjugated polymers (FCPs), such as polyaniline or polythiophene. These FCPs have characteristics of flexibility in molecular design and large absorption cross-section, which make them attractive as signal transducers. (22) Hyperspectral imaging can also be used to detect BPO from flour. It has the ability to find objects, identify materials, and detect processes by obtaining each pixel in the image across the electromagnetic spectrum. (21) Hyperspectral imaging captures both spatial and spectral information, which results in

high data dimensions. However, although large data provides more in-depth details and analysis, it increases the difficulty for analysis of hyperspectral images, such as expensive equipment and knowledge of technique needed.

### **1.3.2 Detection of BA**

For detecting BA, just like BPO, there are calibrations and sample preparations before HPLC injection. Calibration steps are like BPO's. BA was dissolved in methanol to make the stock solution and was further diluted to become a working solution. Appropriate ppm of BA in the solution was correlated with ppm of benzoic acid in flour, from the extraction, to make the standard curve like the area vs ppm of benzoic acid in flour. (8) For BA extraction from flour, it is the same as BPO extraction. At room temperature, diethyl ether was mixed with bleached flour, and the mixture was shaken for 10 minutes and left in repose for 15 minutes. Then, the upper layer of the mixer was extracted and determined by HPLC. The biggest difference for BA detection is that the mobile phase for detecting BA is phosphate buffer/methanol (95:5) due to its polarity.

Gas chromatography (GC) is another common method to detect BA in foods. Like HPLC, GC requires tedious sample preparation before injecting into GC. Dispersive liquid-liquid microextraction (DLLME) (23) is a technique used in GC sample preparation. This technique involves cumbersome steps, including injection, extraction, and centrifugation, which results in the low efficiency for the GC method. Other techniques used in GC are liquid-liquid extraction and solid phase extraction. (24) These two techniques not only have extended preparation time, but also require a huge amount of organic solvent, which results in a possible biohazard to both human and environment.

Other methods for detecting BA are spectrophotometric detection (25), capillary electrophoresis (26), biosensor (27), and room temperature phosphorescence (28). Even though the above methods provided trustable data analysis for BA detection, several drawbacks can be found within those methods. For example, spectrophotometric detection has limited practical use due to its tremendous and complex apparatus.

## **1.4 Raman Spectroscopy and Surface Enhanced Raman**

### **Spectroscopy**

Raman spectroscopy is a technique that analyzes and provides information about chemical structure based on the interaction between light and chemical bonds. (29) Raman Spectrum gives several peaks, which show the intensity and wavelength position of Raman scattering. Each peak represents a specific molecule. The Raman spectrum also provides chemical structure and identity, phase and polymorphism, and contamination and impurity. However, Raman spectroscopy's spectrum has detection limits due to extremely low intensity. Therefore, several techniques were developed to improve the intensity of Raman Spectroscopy.

SERS is a technique that enhances the Raman scattering by molecules adsorbed on rough metal surfaces or by nanostructures, typically gold or silver metal. (11) The mechanisms behind SERS can be explained by either electromagnetic theory or chemical theory. For electromagnetic theory, the Raman signal increases the adsorbate's intensity due to the generation of a large electric field, which is provided by the surface. Rough surface and arrangements of nanoparticles are required for SERS because those surfaces provide areas for localized collective oscillation to occur, which enhanced the signal of Raman scattering. (12) For chemical theory, the enhancement of Raman scattering

intensity is due to the charge transfer between the metal and adsorbate molecules. This charge transfer enhances signal by providing a pathway for resonant excitation. (13) In order for this enhancement to happen, the targeted molecules must be directly adsorbed to the metal surface.

SERS measurement can be performed by two main substrates. One is in colloidal solution, and another is in solid substrates. For colloidal solution, targeted elements are prepared with metal nanostructure on a solid support. Although this type of substrate gives strong sensitivity, its short lifetime caused by metal's surface oxidation and boring procedure limit this substrate type's application. Wet chemical method was then discovered by adding stabilizing agents with colloidal solution-based metal nanostructures. Although the stabilizing agents help to extend the colloidal solution's lifetime, the density of metal nanostructures must be low to prevent coagulation. Low density of nanostructure also means low intensity of SERS result. (15) For the solid substrates method, rough or nanoporous surfaces are typically used as substrates. One common example is porous silicon coated with noble metals. Porous silicon can be obtained by electrochemical etching in hydrofluoric acid. After etching, test samples consist of networks of pores with different diameters and depth, which depends on the etching condition. (14) Because of its high surface-to-volume ratio, this can be used in SERS and other photonic and sensing devices.

Numerous methods were developed to improve the sensitivity for SERS detection. Nowadays, the most common method is by dropping a liquid sample onto a nanostructured noble metal surface, such as gold or aluminum. This method can be explained by the coffee ring effect due to the capillary action and weak Marangoni flow

of the solvent. The sample substrates dropped on metal surface after evaporation will be pushed to the outer surface of the droplet, and pack solute molecules and metal nanostructures close to each other and further strengthen the hotspot effect for SERS measurements.

SERS can be operated either by benchtop or portable. They both have distinguished pros and cons. For benchtop SERS, its advantages include high-powered laser and high spectral resolution of the acquired spectra. (16) Furthermore, samples tested by a benchtop instrument tend to have better signal due to less interference from fluorescence caused by higher excitation wavelengths. Cons for benchtop SERS are its tremendous size and high cost. Due to its size, benchtop SERS usually sits in the lab, which makes it difficult to test field samples. Samples may degrade during the transportation from field to lab. Benchtop SERS can also create safety concerns due to its high-powered laser. For portable SERS, its compact size and affordability are its advantages. It can appear in places like airports or factories due to their convenient portability. However, its disadvantages include fluorescence interferences caused by lower-excitation wavelengths and lower-laser power. (16) Both benchtop and portable SERS have their own pros and cons. Therefore, it is important to use the most suitable one depending on the situation.

SERS detection can be analyzed in both qualitative characterization by peak and quantitative by intensity. SERS measurement provides a graph consisting of Raman shift as X-axis and intensity as Y-axis. For qualitative analysis, it is performed by the analysis of common peak position. (20) In other words, each element or bond has its own and unique peak assignment. Because of this feature, we can recognize the element from a

mixture by whether the mixture has a common peak with the targeted element. We can acquire the target element from either databases or test the element alone. For quantitative analysis, intensity from the SERS graph will be used. The intensity changes proportionally as the concentration of mixture changes. (20) Once we find a linear relationship between intensity and concentration in a certain range, we can use that linear graph to create an equation to calculate back all of the information we want at that range.

SERS can be applied in analytical chemistry due to its convenient and sensitive technique. SERS has the ability to analyze the content in foods to ensure the quality and prevent illegal adulteration in products. (28) SERS is able to trace targeted ingredients from a complex sample, such as flour. (19) Furthermore, SERS can be used to observe catalysis and electrochemistry. For instance, SERS can observe the electron transfer between proteins and membranes at electrodes. (30) Other analytical applications include the direct detection of a solid-phase-bound compound, and SERS detection through external plasmonic nanostructures is an example for this. (30) In addition, using SERS has a huge potential in bioanalytical application. For example, protein detection can be obtained by using SERS fingerprints, including DNA, RNA, and other proteins in tissues. (30)

There was no SERS application yet for quantifying BPO in flour. However, we can figure out the BPO amount in flour by Raman spectroscopy. By using Raman spectroscopy, BPO extracted from flour has two characteristic peaks, which are at  $1001\text{ cm}^{-1}$  and  $1777\text{ cm}^{-1}$ . (31) However, the BPO sample's concentration range in that study is from 0.05% to 1%, which is not practical since the regulation for BPO in flour is no greater than 40ppm. On the other hand, SERS has been applied to BA detection already.

With the technique that was prepared by vacuum depositing silver on silica nanospheres, the SERS sensitivity and the signal of BA increased as the silver-film became thicker.

(32) BA was then distinguished by characteristic peaks at  $1003\text{ cm}^{-1}$  and  $1600\text{ cm}^{-1}$ . The detection limit for BA was  $5 \times 10^{-7}\text{ M}$ . (32)

## 1.5 Goals and Objectives

In this research, I aim to develop a rapid and cost-effective determination for benzoyl peroxide by SERS with a Raman device to replace current methods. The reason is that current methods, such as HPLC, have complex sample preparation, are costly, and require lengthy testing time. Another reason is that the current method, hyperspectral imaging, requires complex data analysis. In addition, even though Raman spectroscopy had the ability to detect the BPO concentration, the detection limit range was not in the regulation. To achieve these goals, these are objectives for this research.

Objective 1 is to develop and optimize a detection method for BPO and BA by SERS. By using SERS, BPO and BA were mixed with silver nanoparticles to enhance the signal for Raman Spectroscopy. These procedures and techniques are faster than using HPLC. Thus, I believe that SERS can improve the lengthy testing time for current methods.

Objective 2 is to develop a separation method for BPO from flour product without converting to BA and detect in SERS. Sample preparation for HPLC has the possibility to make BPO convert to BA, which will give a false result. My hypothesis is that SERS sample preparation developed in this objective can prevent the conversion of BPO and have more accurate results compared to HPLC's result.

## CHAPTER 2

### DEVELOPMENT OF A DROPLET METHOD FOR RAMAN SPECTROSCOPY TO QUANTIFY BENZOYL PEROXIDE AND BENZOIC ACID

#### 2.1 Introduction

Benzoyl peroxide (BPO) is a strong oxidant that is used as food additive or medical use. When used in flour, BPO acts as a bleaching agent oxidizing the carotenoid to remove yellow color. When used for medical purposes, BPO increases skin turnover, clears pores, and eliminates bacterial count. Thus, BPO has been used as an acne treatment. (33) However, excessive BPO addition can result in damage for flour's existing nutrients, such as carotenoid, vitamin A, vitamin E, and others. (34) Short term over-intake of BPO can cause nausea, dizziness, and neurasthenia in humans. (35) Long term consumption of BPO will cause neuritis or angular cheilitis disease, and it may cause accumulative harm to the central nervous system and liver. (34) Therefore, it is necessary to regulate the usage of BPO in food products. In 2009, Codex Alimentarius Commission had determined that the amount of BPO allowed in wheat flour cannot be greater than 75 mg/kg. (36)

BPO is extremely unstable and can easily convert to Benzoic Acid (BA) (figure 4). Current methods for detecting BPO are high-performance liquid chromatography (HPLC) and spectrophotometry. However, these methods have limitations. Both HPLC and spectrophotometry measure BA's concentration and calculate back to obtain BPO's concentration because BPO converts to BA during sample preparation (Figure 5). This is a considerable drawback for current methods because BA can be added as a food preservative. (37) Hence, it is difficult to quantify the original BPO's concentration if

there was BA originally in food products. In addition, both methods require considerable sample preparation steps for detection in flour. (35)

Raman spectroscopy is a technique based on the inelastic Raman scattering of photons by matter. (38) (39) In a Raman spectrum, the characteristic peaks can be used to identify specific molecules or bonds, and the intensity is correlated to the concentration of target molecules or compounds. (34) A limitation for Raman spectroscopy is weak scattering, which results in low intensity. One technique to enhance its low intensity is surface-enhanced Raman spectroscopy (SERS). SERS is an integration of Raman spectroscopic technique that uses its nanotechnology to create a stronger Raman scattering that enhances the intensity. SERS improves the sensitivity greatly and thus has gained more attention nowadays, and is widely used in detection of food additives. (40) (41) (42) (43) With the mineralization of the Raman instrument, this technique is more portable and cost-effective than HPLC or spectrophotometry.

In this study, we investigated the normal Raman spectroscopy and SERS to detect and quantify BPO and BA, respectively. Their capabilities and limitations were discussed.

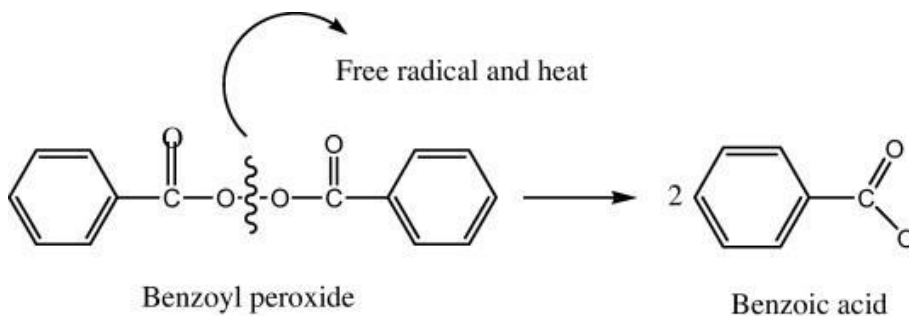


Figure 4: decomposition mechanism of BPO.

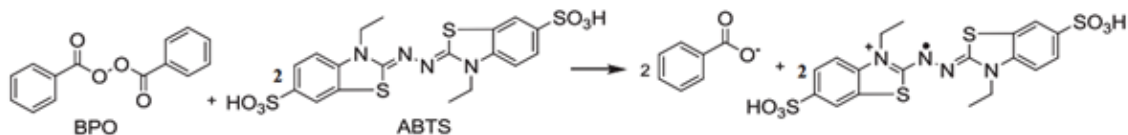


Figure 5: possible reaction of BPO for spectrophotometry.

## 2.2 Material and methods

### 2.2.1 Materials

>98% reagent grade Benzoyl Peroxide and >99.5% reagent grade Benzoic acid were purchased from MilliporeSigma, Inc. (Burlington, MA) HPLC grade acetonitrile, Ted Pella Inc Parafilm M, and 99.5% Butylated hydroxytoluene (BHT) were purchased from Thermo Fisher Scientific. (Madison, WI) 50 nm Silver Nanospheres with citrate coating was purchased from Nanocomposix (San Diego, CA). Aluminum foil was purchased from local WAL-MART in Amherst, MA.

### 2.2.2 Substrate and sample preparation

#### 2.2.2.1 Normal Raman

BPO/BA solutions were prepared by mixing BPO/BA crystal with HPLC grade acetonitrile. This solution was vortexed briefly. 2  $\mu$ l of solution (1000 ppm) was dropped on an aluminum surface slide and air dried for Raman analysis.

#### 2.2.2.2 SERS

For SERS sample preparation, two different metal nanoparticles were used, AgNPs (50 nm) or AuNPs (50 nm). Nanoparticles were mixed with BPO/BA solution at 1:1 ratio. After the mixture was pipetted back and forth a few times and vortexed, 2  $\mu$ l of mixture was dropped on an aluminum surface plate and air dried to form

a distinct ring of nanoparticles showing around the edge of the droplet. This area is referred to as 'coffee ring'. (44) The high concentration of nanoparticles in this area gives higher Raman intensity compared to the rest of the droplet. Hence, this area was chosen for Raman analysis.

### **2.2.2.3 SERS+antioxidant**

100 ppm of BHT solution was prepared with acetonitrile as solvent. BHT, a strong antioxidant, was added during the SERS sample preparation to see whether it prevented BPO conversion to BA. For the control group, 250  $\mu$ l of BPO/BA solution was mixed with 250  $\mu$ l HPLC grade acetonitrile. For the experimental group, 250  $\mu$ l of BPO/BA solution was mixed with 250 $\mu$ l of 100 ppm BHT solution. This control group was to ensure that the concentration stayed the same as the experimental group. Both control and experimental groups were mixed with 50 nm AgNPs at 1:1 ratio and vortexed. 2  $\mu$ l of sample mixture were dropped on an aluminum plate and formed coffee-rings for Raman analysis.

### **2.2.2.4 Normal Raman (parafilm surface +running method)**

BPO/BA solution was prepared by mixing BPO/BA crystal with acetonitrile. A hydrophobic surface was created by wrapping parafilm over the aluminum plate. 1  $\mu$ l of BPO/BA solution was dropped on the parafilm surface plate. Another 1  $\mu$ l of solution droplet was dropped on the same spot after the previous droplet dried to increase the concentration. This step was repeated two more times and resulted in a total of 3 droplets for each sample. After the last droplet dried, 15 spectra were collected from three random areas within the dried droplet. This procedure was repeated two times for each concentration for establishing a standard curve.

### 2.2.3 Raman analysis

A Thermo Scientific DXR Raman microscope was used for all normal Raman and SERS measurements. (Thermo Fisher Scientific, Waltham, MA) An excitation wavelength of 780 nm was used, with a laser power of 20 mW and exposure time of 1 second for normal Raman and 5 mW and exposure time of 1 second for SERS. The reading between  $2000\text{ cm}^{-1}$  and  $400\text{ cm}^{-1}$  were analyzed for comparison between BPO and BA. For the standard curve, the peak height at  $1780\text{ cm}^{-1}$  was analyzed for BPO, and the peak height at  $800\text{ cm}^{-1}$  was analyzed for BA. (45) (46) Microsoft Excel Worksheet software was used to obtain average spectra, variation, and further statistical analysis for standard curves.

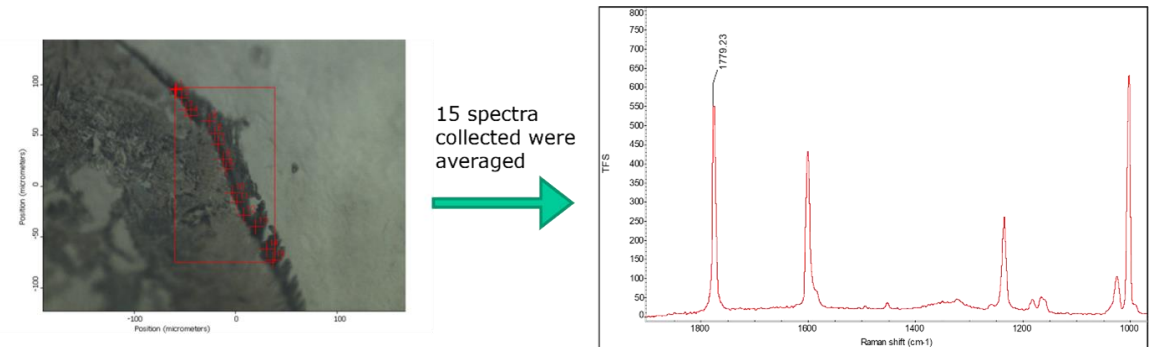


Figure 6: demonstration of BPO Raman analysis. Peak at  $1780\text{ cm}^{-1}$  is used to create standard curves.

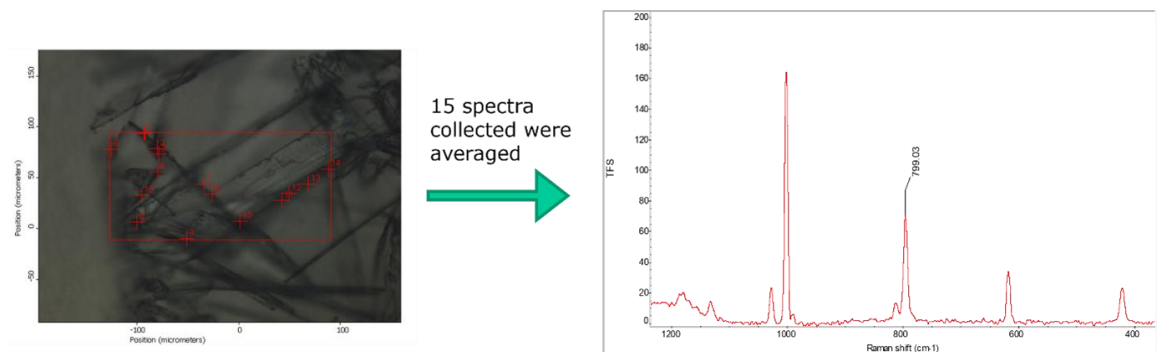


Figure 7: demonstration of BA Raman analysis. Peak at  $800\text{ cm}^{-1}$  is used to create standard curves.

## 2.3 Result and discussion

### 2.3.1 Normal Raman (aluminum surface)

To distinguish between BPO and BA, it is necessary to figure out their peak assignment and observe the difference between them. 1000 ppm of BPO and BA were tested. As shown in figure 8, there are several distinguished peaks between BPO and BA. For instance, peaks at  $1780\text{ cm}^{-1}$ ,  $1600\text{ cm}^{-1}$ , and  $1232\text{ cm}^{-1}$  can be used to identify BPO. Peak at  $800\text{ cm}^{-1}$  can be used to identify BA. (45) (47) Although this Raman method differentiates between BPO and BA, the intensities are too low to achieve the regulation concentration, which is 75 ppm. Further methods are developed to enhance this weak Raman scattering.

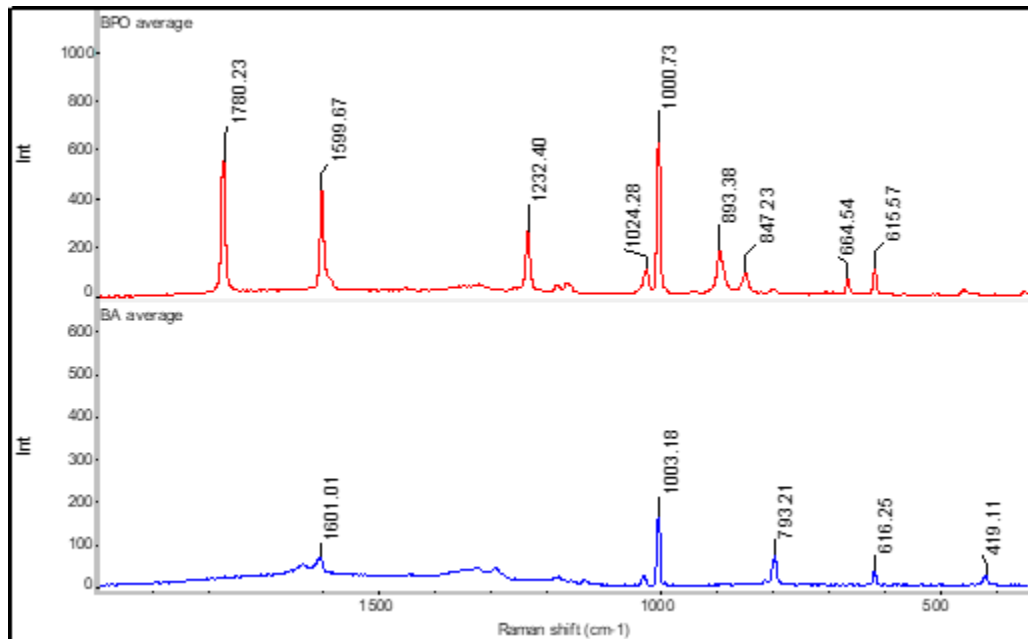


Figure 8: average Raman spectra for 1000 ppm of BA and BPO.

### 2.3.2 SERS

Figure 9 provides the average spectra for 100 ppm of BPO with AgNPs. The results show the overall SERS intensities were much higher than those in the normal Raman spectra, the SERS characteristic peaks between BPO and BA were very similar. This might be due to the decomposition of BPO. During the SERS sample preparation, BPO was too unstable and converted into BA (Figure 4). This explains why SERS's BPO and BA spectra (Figure 9) are like normal Raman's BA spectra (figure 8).

Although visually the BPO and BA's SERS spectra look like each other, using principal component analysis (PCA), we were able to achieve 85% accuracy for identifying BPO and 90% accuracy for BA. This was estimated based on the approach that used randomly selected 70% of all BPO/BA data to establish a PCA model and predicted the remaining 30% data (Figure 10). However, it is still challenging for quantitative analysis as they share the same peaks. A possible solution is to add the antioxidant to prevent the BPO oxidation to BA.

Figure 11 showed the average SERS spectra with the AuNPs for 100 ppm of the BPO and 100 ppm of the BA. Similar to the AgNPs result (Figure 9), AuNPs did not prevent the BPO's degradation either. BPO lost its characteristic peaks and showed similar peak assignments compared to BA. This might be due to the great surface area of the AuNPs, which functioned as a catalyst and allowed BPO converting to BA.

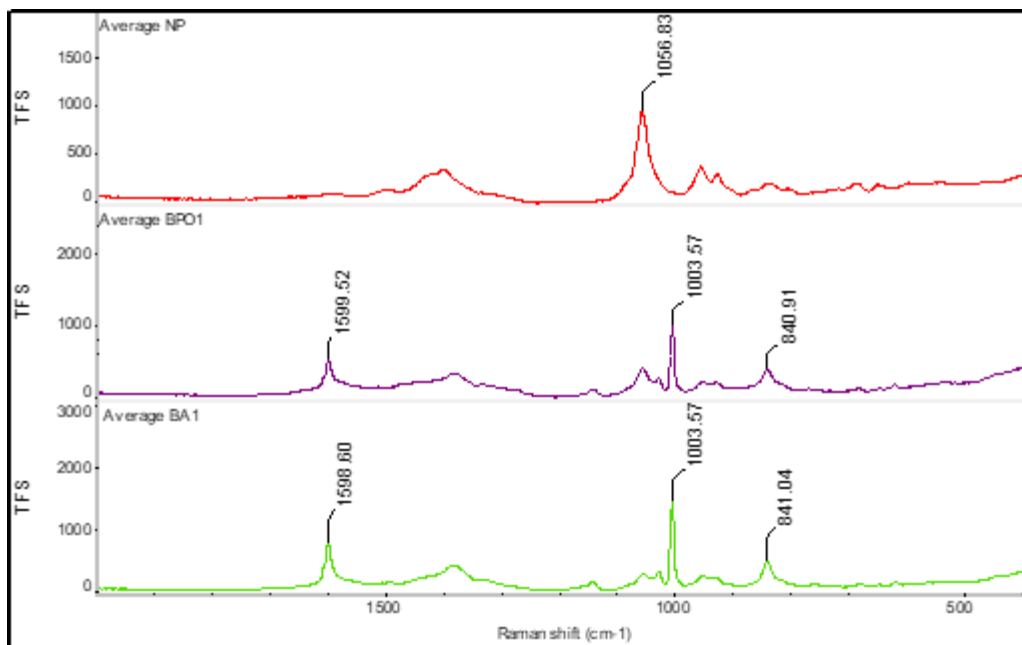


Figure 9: average Raman spectra of AgNPs, 100 ppm of BPO with AgNPs, and 100 ppm of BA with AgNPs.

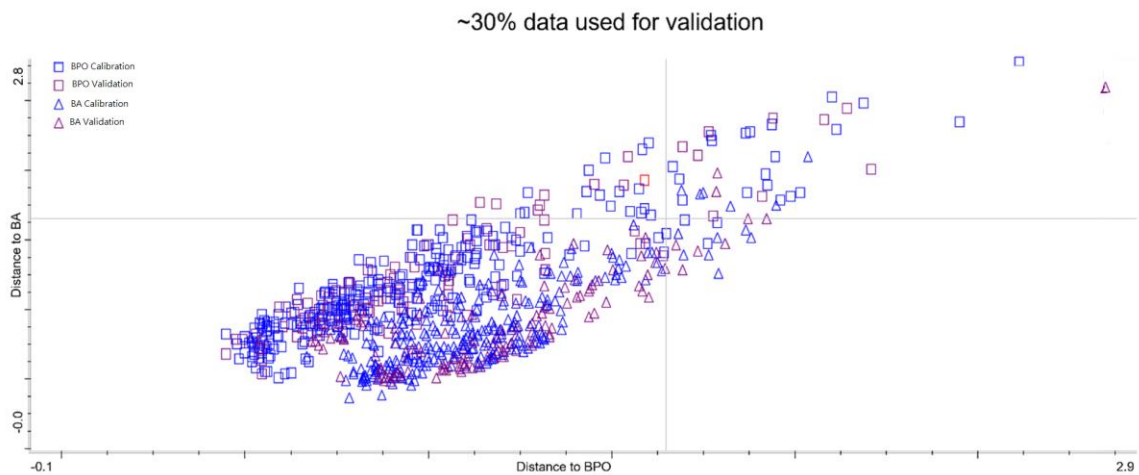


Figure 10: PCA result for BPO and BA with SERS. 70% of data were used for model establishment, and 30% of remaining as validation. BPO accuracy is 85%. BA accuracy is 90%.

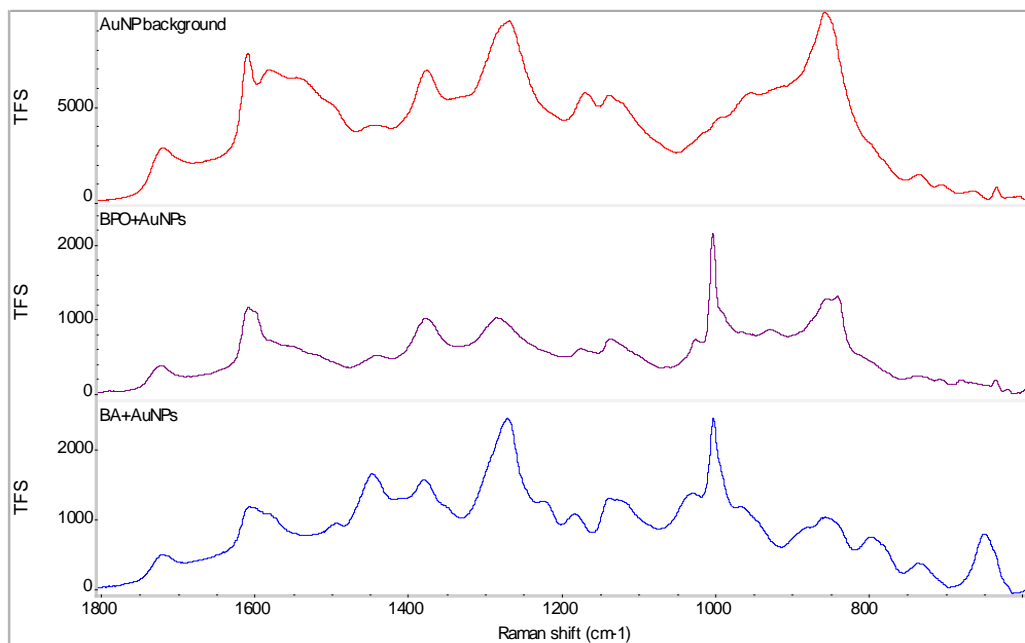


Figure 11: average Raman spectra of AuNPs, 100 ppm of BPO with AuNPs, and 100 ppm of BA with AuNPs.

### 2.3.3 SERS +antioxidant

As shown previously, BPO converted to BA during the SERS sample preparation. The conversion probably happened during the AgNPs addition. So, BHT was added with the BPO before mixing with AgNPs to see if BHT would prevent the oxidation of BPO to BA. Figure 12 shows that there is hardly any peak difference between BPO and BA even after adding BHT. Hence, BHT cannot prevent BPO oxidation during the SERS sample preparation. Figure 13 delivers the relationship for BPO and BA with or without BHT. There is no trend among four batches. BPO's intensity in batch 1 and 2 decreased after adding BHT, but it increased after BHT addition in batch 4. Same relationship happens to BA. There is no trend for BHT addition affecting the intensity of BPO and BA.

Therefore, SERS with antioxidant addition cannot be used to differentiate between BPO and BA.

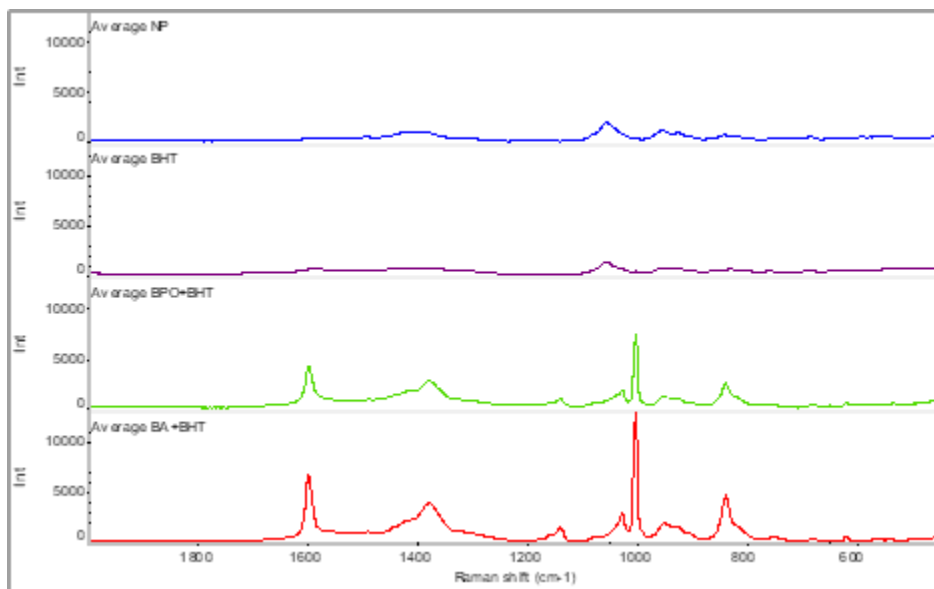


Figure 12: SERS Raman spectra of AgNPs, 100 ppm of BHT, BPO+BHT, and BA+BHT.

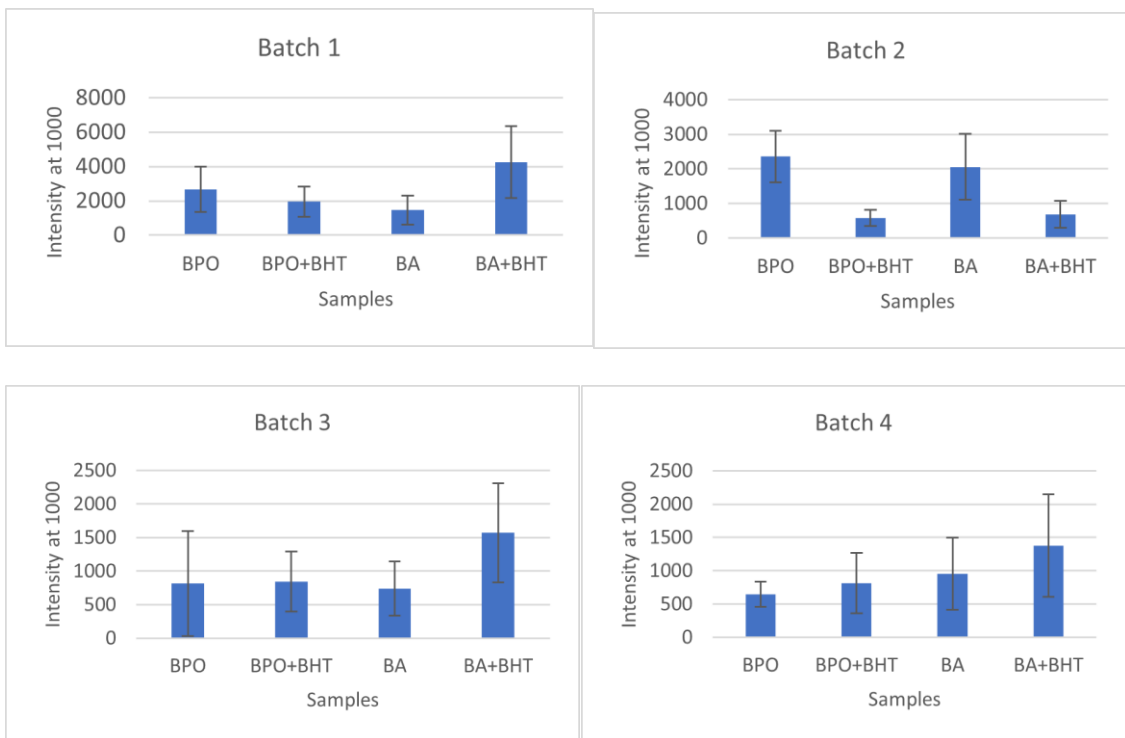


Figure 13: four batches of SERS intensity at  $1000\text{ cm}^{-1}$  produced from 100 ppm of BPO and BA with or without BHT. Error bars represent the standard deviation of the average signal intensity at  $1000\text{ cm}^{-1}$ .

### **2.3.4 Normal Raman (parafilm surface +running method)**

Since the SERS methods did not work at quantifying BPO discriminating from BA, we went back to further explore the normal Raman and see whether we could improve the sensitivity of normal Raman with using the AgNPs. Here we presented a new method which used a hydrophobic surface to reduce the spread of the droplet and thus to concentrate the droplet concentration during the drying process. As shown in figure 14A, acetonitrile did not hold the droplet on the aluminum plate surface due to low surface tension. The droplet spread out immediately once dropped. In addition, it was difficult to locate acetonitrile droplets on aluminum surface, especially in low concentration. A parafilm surface was created for acetonitrile droplet. By using parafilm surface, BPO samples held droplets instead of spreading apart (Figure 14B). It resulted in smaller droplet, which helped to locate and collect spectra easier. Thus, it improved the visibility and intensity.

Figure 15 showed the standard curves for BPO concentration at  $1780\text{ cm}^{-1}$ . It gave a linear relationship range from 250 ppm to 25 ppm. Three different stocks of BPO solution were tested on 3 independent days, and proved that normal Raman with running method on parafilm surface provided consistent results for BPO's standard curve. The limit of detection was estimated to be 25 ppm (Figure15A, 15B, 15C). In addition, this method not only prevented BPO conversion, but also largely reduced the sample preparation time and detection time compared to the HPLC method. (35)

Figure 16 provides the standard curves for BA concentration at  $800\text{ cm}^{-1}$ . For BA, 1000 ppm to 250 ppm was tested because it had regulation limiting at 0.1% by weight, which was 1000 ppm. From 1000 ppm to 250 ppm, this method provided an acceptable standard curve and consistent results in two independent testing of BA (Figure 16D, 16E).

To further improve the sensitivity for applying the Raman spectroscopy for flour sample analysis, we also explored the Raman mapping using a more advanced Raman microscope (DXRxi) which is capable of collecting hundreds of spectra in a short time and more sensitively. As shown in Figure 15A2, 15B2, 15C2, 16D2, and 16E2, the Raman image of 75 ppm BPO and 500 ppm BA showed much higher intensity and the map result also indicated the distribution of the target analyte to provide better visual observation on the analysis. Therefore, in chapter 3, we used the image analysis instead of spectral analysis to further evaluate the Raman spectroscopy for BPO detection in the flour sample. More details of image analysis will be discussed in the next chapter.

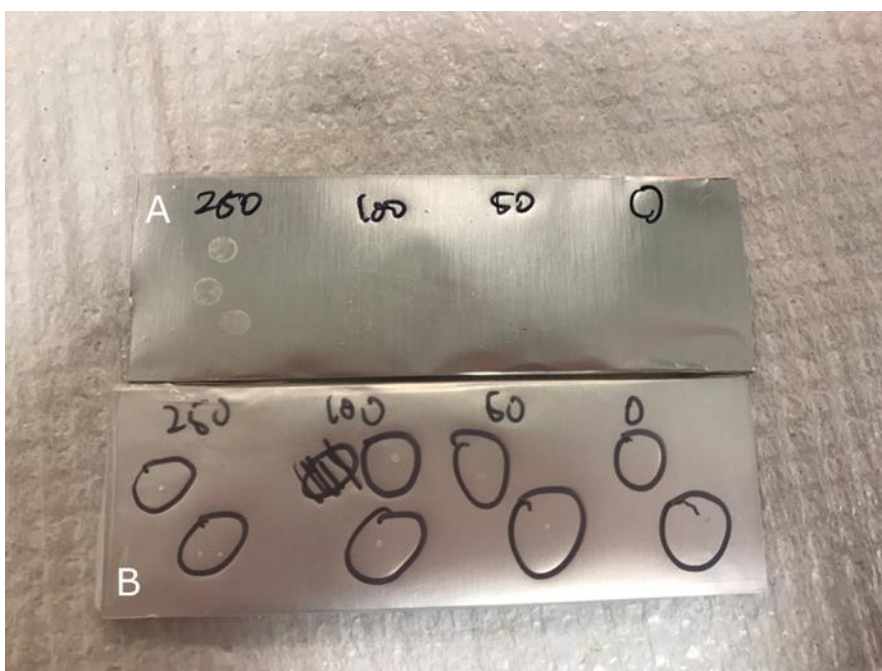
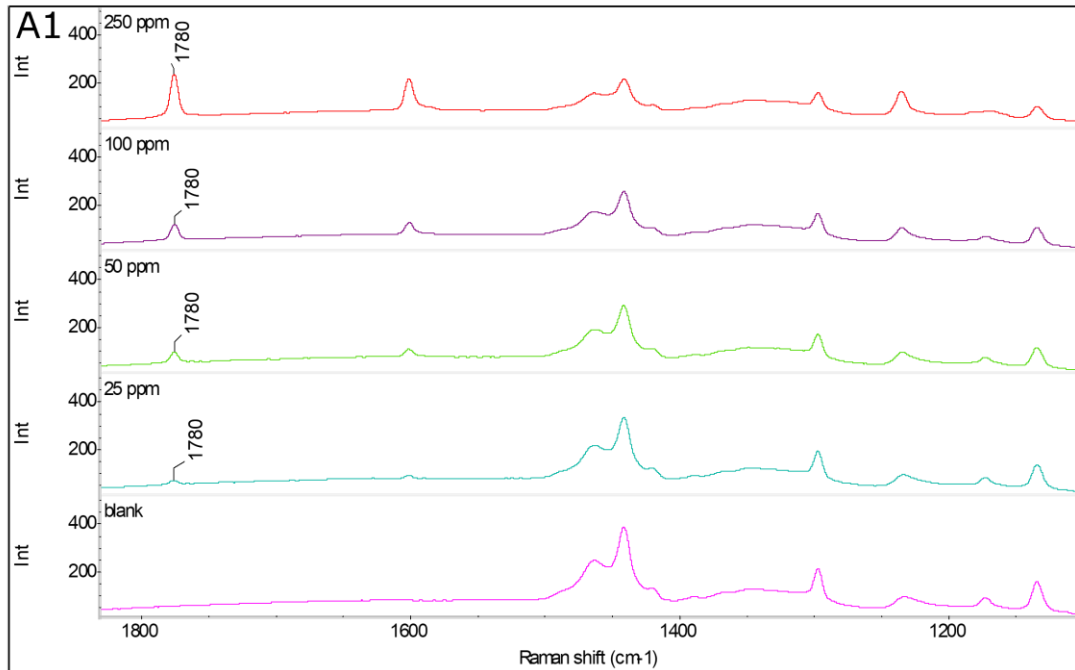
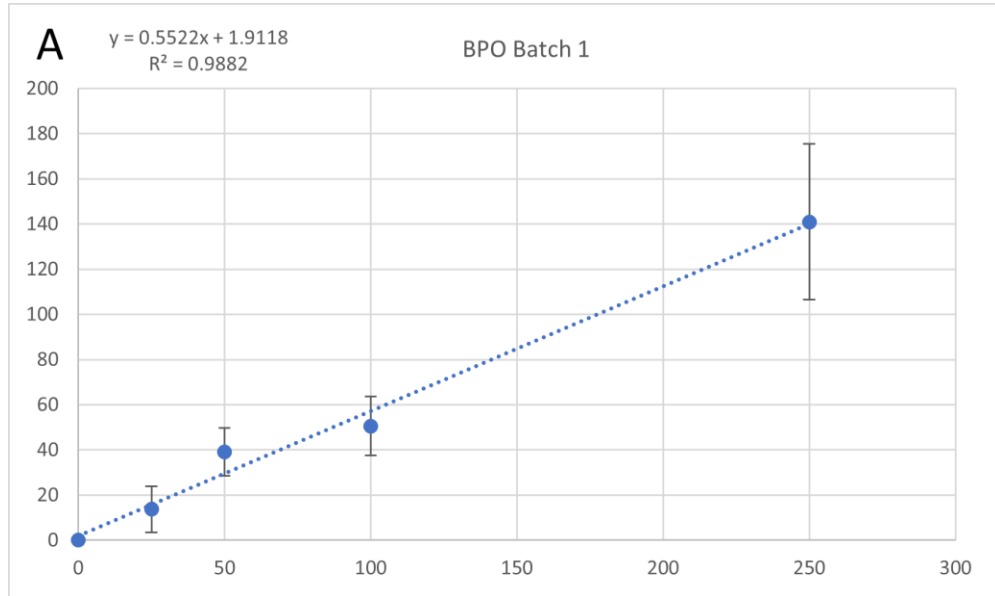
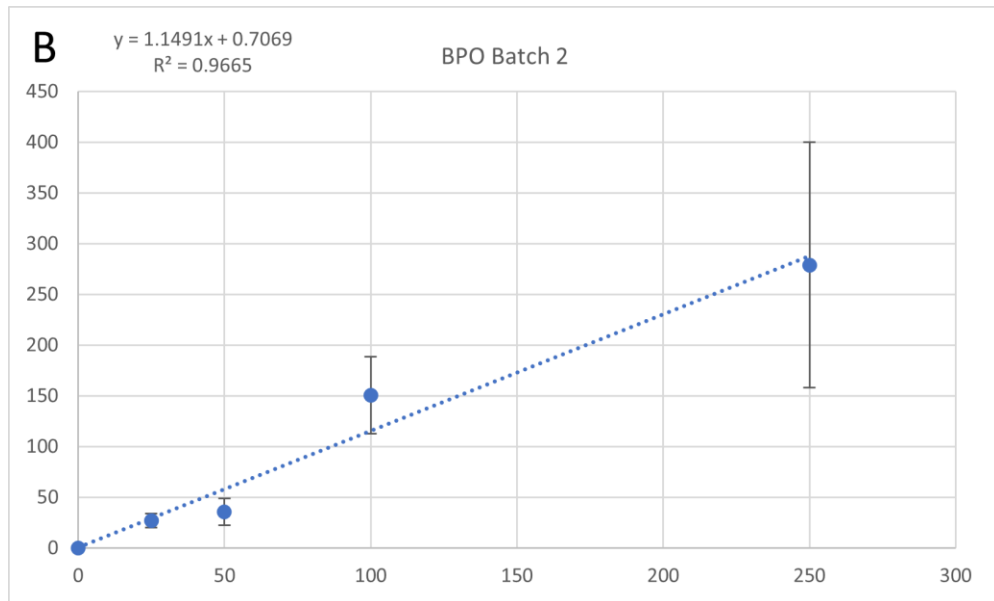
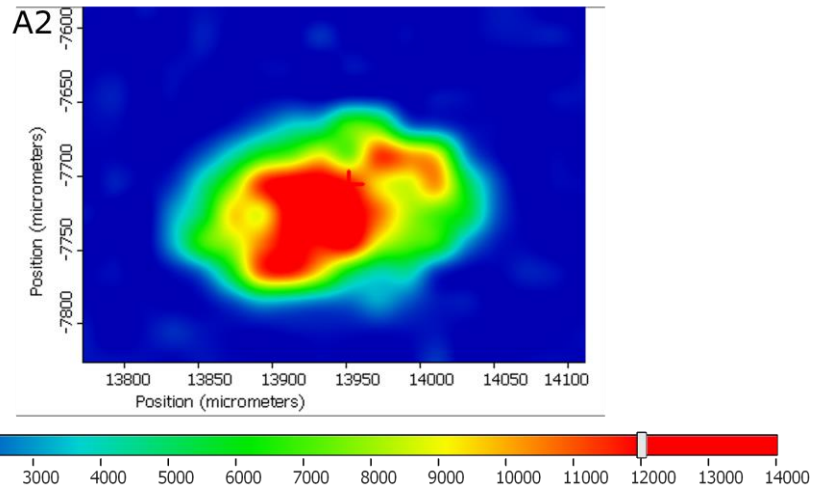
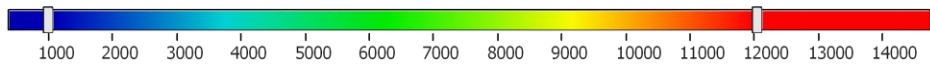
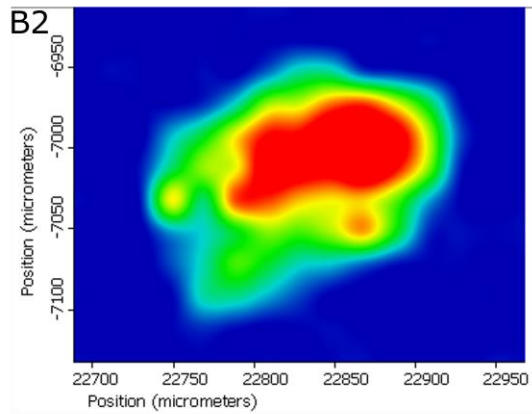
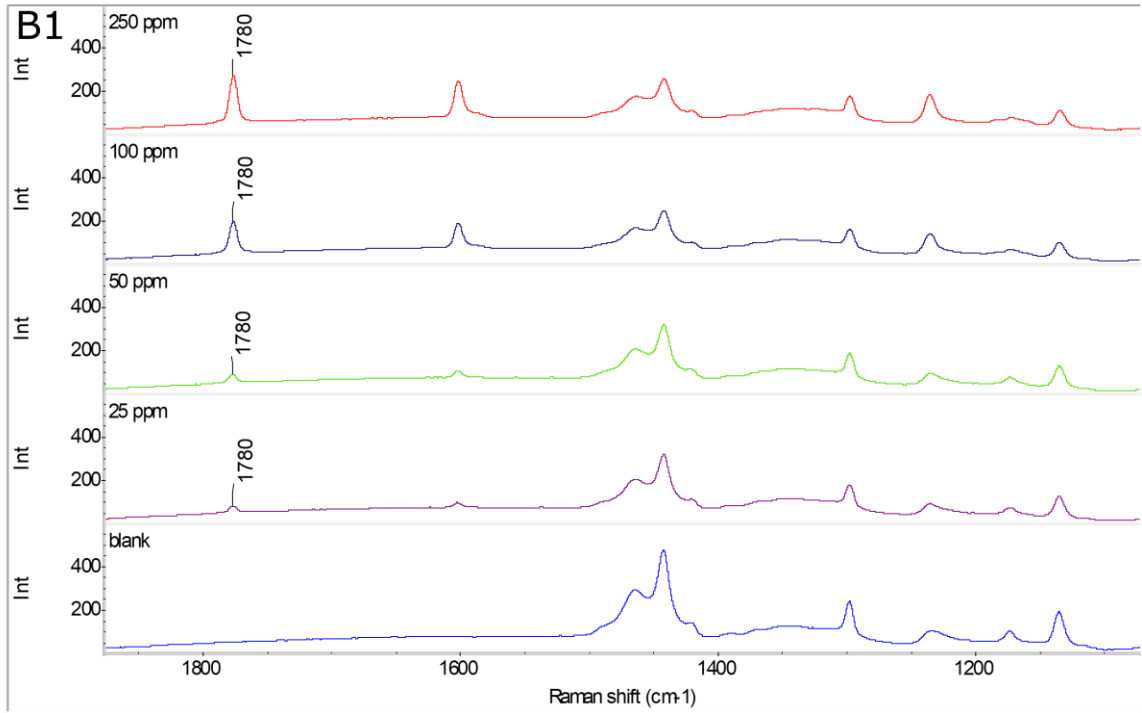
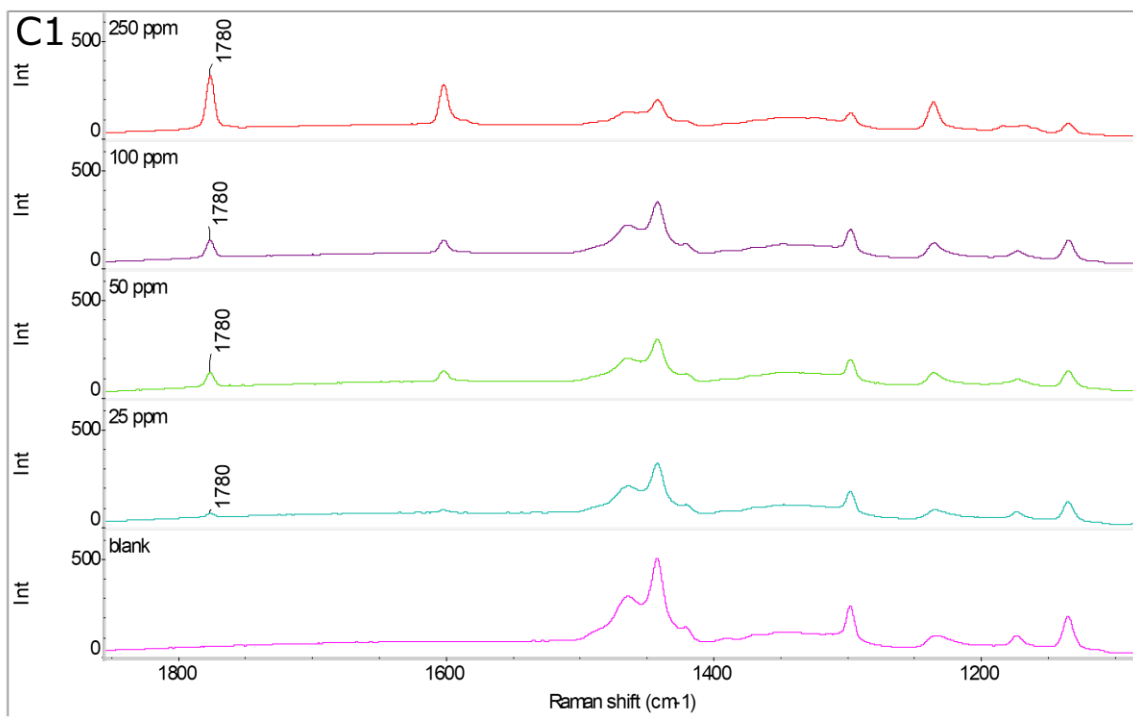
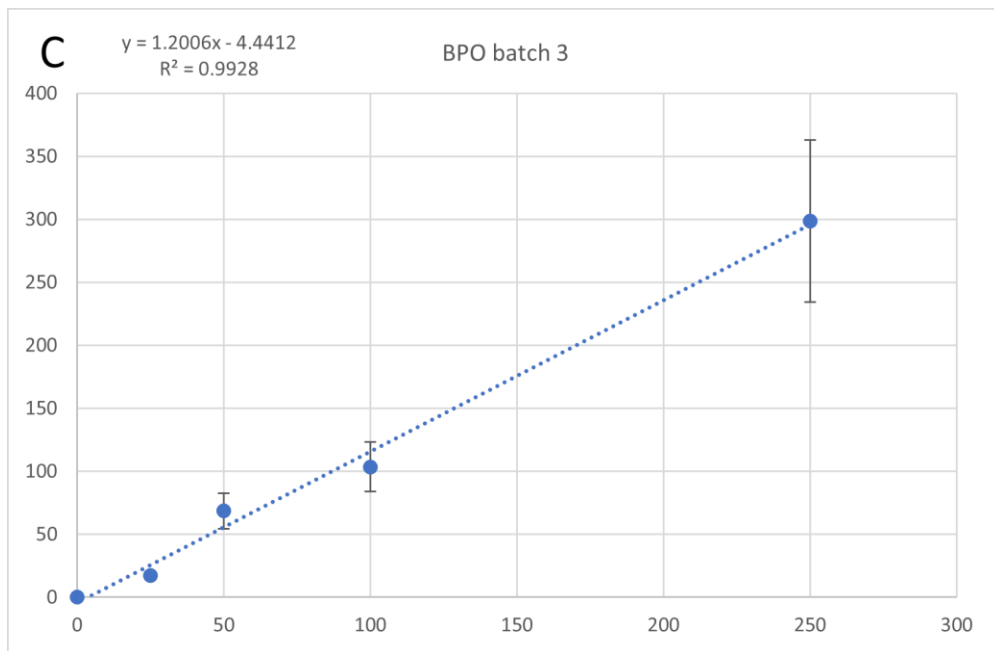


Figure 14: (A) BPO droplet on aluminum plate. Droplet for 100ppm or lower barely observable (B) BPO droplet on parafilm surface. Aggregate substrate, easy to observe.









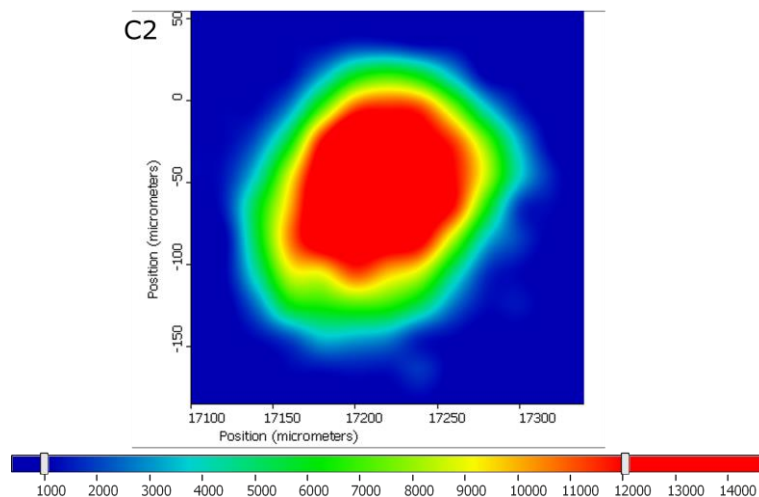
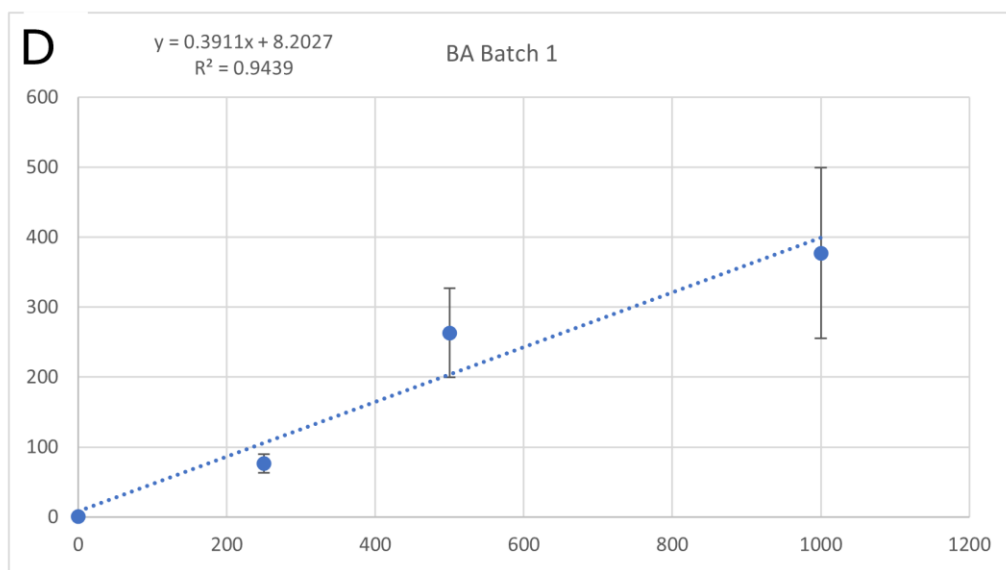
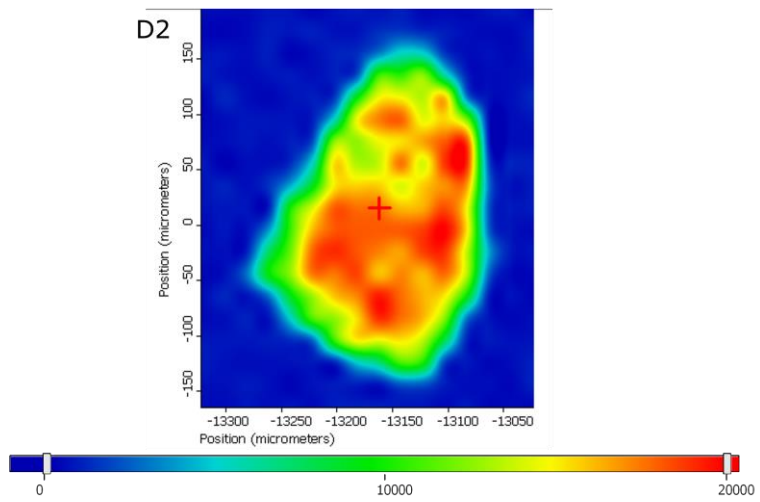
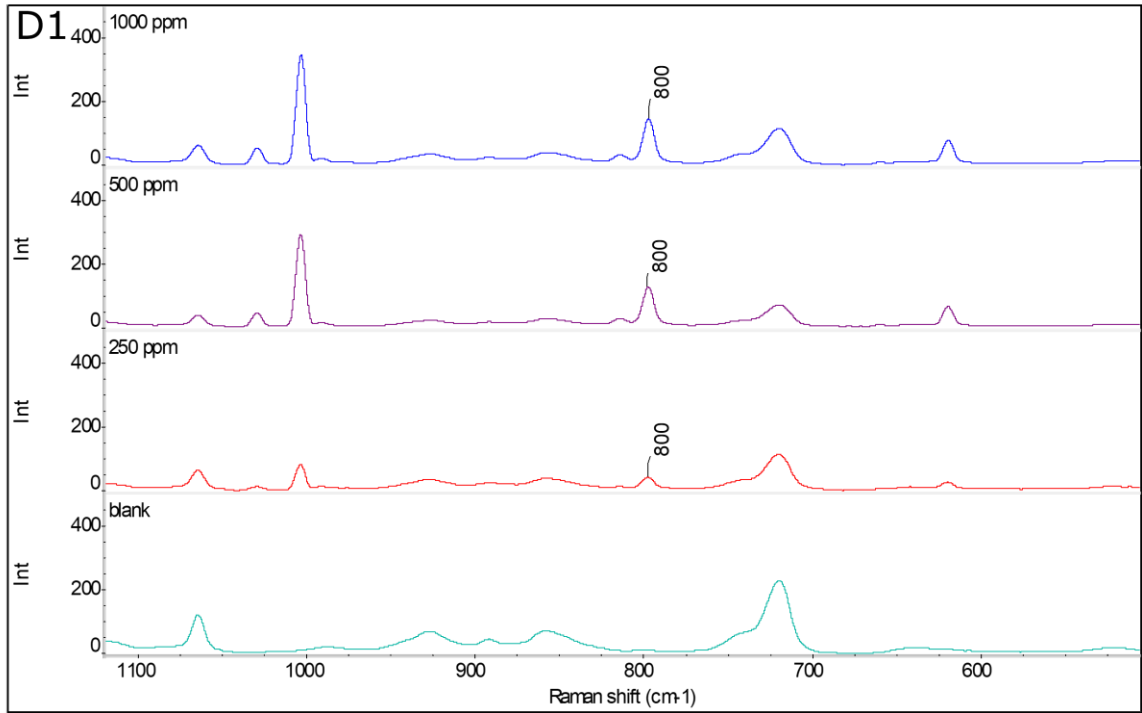
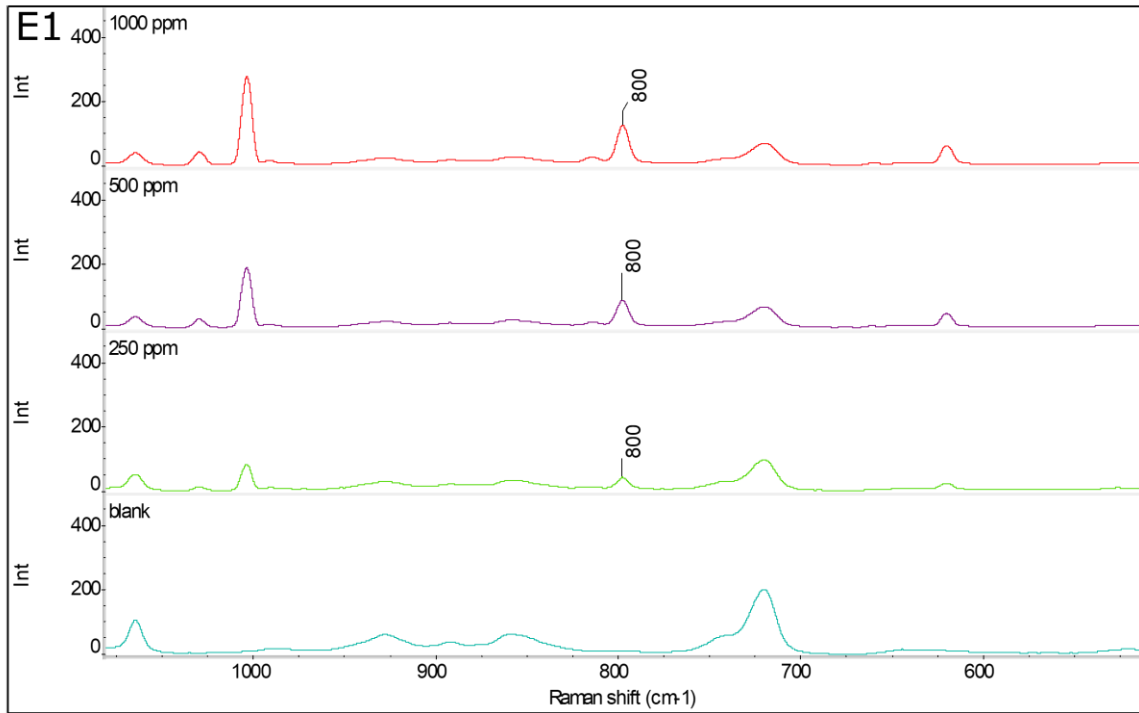
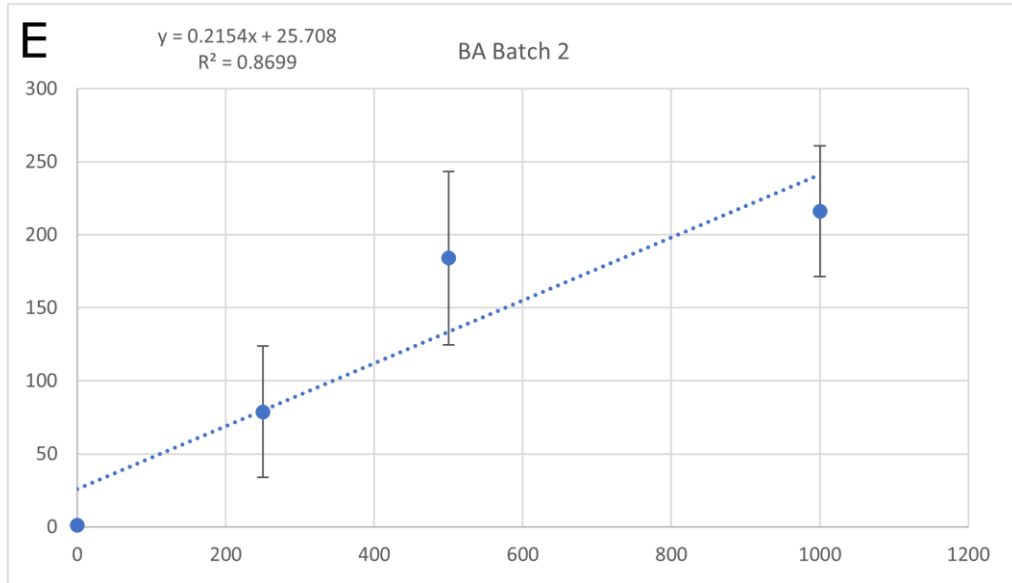


Figure 15: standard curve of BPO concentration produced from the average Raman intensity at  $1780\text{ cm}^{-1}$ . Error bars represent the standard deviation of average signal intensity at  $1780\text{ cm}^{-1}$ . (A) (B) (C) represent three different batches of stock BPO tested. (A1) (B1) (C1) represent Raman images of average 25, 50, 100, and 250 ppm of BPO corresponding to (A) (B) (C). (A2) (B2) (C2) represent the 75 ppm BPO's DXRxi Raman image corresponding to (A) (B) (C)







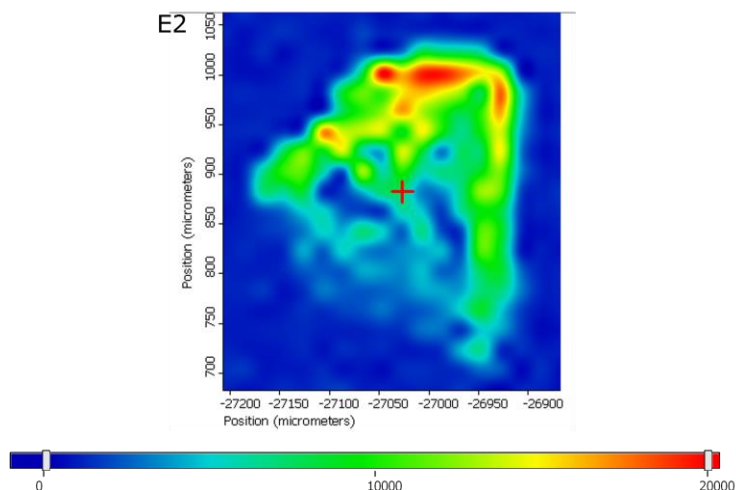


Figure 16: standard curve of BA concentration produced from the average Raman intensity at  $800\text{ cm}^{-1}$ . Error bars represent the standard deviation of average signal intensity at  $800\text{ cm}^{-1}$ . (D) (E) represent two different stocks of BA were being tested. (D1) (E1) represent Raman images of average 250, 500, and 1000 ppm of BA corresponding to (D) (E). (D2) (E2) represent the 500 ppm BA's DXRxi Raman image corresponding to (D) (E)

## 2.4 Conclusion

In this study, we have evaluated various Raman spectroscopic methods to detect BPO and BA. For normal Raman spectroscopy, BPO and BA showed different peak characteristics, which can be used to differentiate them. However, the intensities were too weak to obtain regulation concentration. By using SERS with either AgNPs or AuNPs, the intensity improved significantly. However, BPO converted to BA, which resulted in visually undistinguished SERS spectra between BPO and BA. Although BPO and BA can be distinguished by PCA, it is difficult for quantitative analysis. Further exploration using an antioxidant BHT during the SERS sample preparation did not prevent the BPO degradation, and it did not create an intensity change pattern either. After that, we came

back to the normal Raman approach and focused on improving the normal Raman signals without using AgNPs. With the use of a hydrophobic surface (i.e., parafilm), and repeating droplet method, we were able to concentrate the solution and lower the detection limit of BPO to around 25 ppm which was below the regulation limit of 75 ppm. Standard curves were established for both BPO and BA in the range of 250 ppm to 25 ppm for BPO and 1000 ppm to 250 ppm for BA, respectively. In the next chapter, we explored a method to preliminarily detect the range of BPO concentration in flour samples with image analysis.

## CHAPTER 3

# EVALUATE THE FLOUR MATRIX EFFECT ON BPO DETECTION IN FLOUR SAMPLES

### 3.1 Introduction

Wheat is a major human food source that is consumed worldwide. Flour is one of major processed wheat products, and it is made by grinding raw wheat into powder. Flour appears pale yellow color due to the lutein in wheat and whiten over time. (49) However, consumers care about the appearance of flour, and manufacturers do not have time for the slow whitening process. Bleaching agent was added to flour to accelerate the whitening process. One common bleaching agent is BPO. In addition, freshly milled wheat flour has a high viscosity and absence of flexibility, which does not make it suitable for bakery products. (50) By adding BPO, this freshly milled flour will ripen and improve this condition. This step is also known as aging or maturing.

However, excessive BPO addition in wheat flour can destroy some existing nutrients, such as tocopherol and carotene. (50) Long-term consumption of bleached flour can cause vitamin deficiency, resulting in certain diseases, such as neuritis. (48) Over-consumption may cause cumulative damage to the human body, such as liver failure. Therefore, some countries have brought attention to the usage of BPO in food products. In the United States, the FDA had stated that BPO is generally recognized as safe according to the code of federal regulation, but WHO suggested daily dosage of only 40 mg/kg (51). In Japan, diluted BPO is allowed as an additive in flour, and the regulation permits the use of diluted BPO (19%-22% w/w) in flour for less than 0.3 g/kg. (52) In

other countries, China and France had strictly prohibited the usage of BPO in wheat flour. (52) (53) According to the codex of Alimentarius Commission, BPO's regulation in wheat flour is 75 mg/kg, which is 75 ppm. (55)

There are several methods developed for analyzing BPO in wheat flour, such as HPLC and spectrophotometry. These methods have limitations, which is that they cannot precisely measure the BPO content in wheat flour. HPLC's sample preparation converted BPO in flour into BA by adding potassium iodide. (50) Spectrophotometry introduced ABTS and converted BPO in BA during the sample preparation. (56) The BA concentration was collected and calculated back to trace BPO amount by both methods. This is a significant drawback since BA can be added as a food preservative. By using HPLC or spectrophotometry, it is difficult to identify the exact BPO concentration if the sample contains both BPO and BA.

In this study, the flour matrix effect for BPO in flour samples was discussed, and a rapid and simple extraction method for BPO in flour was developed and detected by Raman spectroscopy, in which BPO did not convert to BA during the sample preparation. The results indicated a 60% recovery percentage by the extraction method described in this study. Hence, this method may apply to quantify precise BPO concentration for samples that contain both BPO and BA.

## **3.2 Materials and methods**

### **3.2.1 Materials**

>98% reagent grade Benzoyl Peroxide was purchased from MilliporeSigma, Inc. (Burlington, MA) HPLC grade acetonitrile, C18 SPE spin column, and Ted Pella Inc

Parafilm M were purchased from Thermo Fisher Scientific. (Madison, WI) Aluminum foil and unbleached flour were purchased from local WAL-MART in Amherst, MA.

### **3.2.2 Substrate and sample preparation**

#### **3.2.2.1 *In situ* method**

BPO crystal was grinded into fine powder and mixed with unbleached flour to create flour samples. 5%, 2%, 1%, 0.5%, and 0.1% of BPO flour samples were prepared. A ball mill machine was used to mix these samples. Flour samples were mixed at 500 rpm for 10 minutes and was shook for another 5 minutes. 4 grams of mixed flour samples were put into a press machine and pressed into a pellet with 10 tons pressure for 1 minute. An area mapping of the pellet sample was detected by a Thermo Scientific DXRxi Raman Spectro-microscope.

#### **3.2.2.2 Extraction method**

Flour samples made in *in situ* method were tested. 1 gram of mixed flour samples were mixed with 3 ml of acetonitrile. 1 ml of mixture was centrifuged in 10000xg for 5 minutes, and supernatant was extracted. 1  $\mu$ l of extracted supernatant was dropped on a parafilm surface and air dried. Another 1  $\mu$ l of supernatant was dropped after the previous droplet dried and was repeated for a total 3 times. (3X droplet method) The dried droplet was detected by DXRxi Raman under the same condition in *in situ* method.

Extraction method was improved by evaporating the supernatant. After the flour acetonitrile mixture was centrifuged, 1000  $\mu$ l of supernatant was extracted and evaporated in Vacufuge plus at 30°C for 30 minutes. The residue, roughly 200  $\mu$ l, was

vortexed and performed 3X droplet method. The sample's droplet mapping was collected by DXRxi Raman and analyzed with image analysis.

Extraction method was further improved with evaporating step and SPE column. 0.1% of BPO flour sample was used here. After the BPO flour mixture was centrifuged, 1000 $\mu$ l of supernatant was extracted and ran through the C18 SPE spin column. Then, the supernatant was evaporated in Vacufuge plus at 30°C for 30 minutes, and the residue was vortexed. Following the 3X droplet method, the sample's droplet mapping was collected and analyzed by DXRxi Raman.

A spiking BPO procedure was processed to test if the BPO escaped during the evaporating step and to compare the recovery percentage from extracting BPO originally in flour. 1 gram of unbleached flour was mixed with 3 ml acetonitrile. The mixture was then centrifuged, and the supernatant was extracted. The BPO solution was added into the supernatant to create 75 ppm of BPO (testing whether BPO escaped) and 1000  $\mu$ l of 0.1% BPO (recovery percentage purpose). This 1000  $\mu$ l sample was put into Vacufuge plus at 30°C for 30 minutes. After the evaporating step, the residue was vortexed and performed 3X droplet test. The sample's droplet mapping were collected by DXRxi Raman Imaging Microscope.

### **3.2.3 Raman instrumentation and image analysis**

A Thermo Scientific DXRxi Spectro-microscope was used to collect all Normal Raman's mapping measurements. (Thermo Fisher Scientific, Waltham, MA) Both *in situ* and extraction method's data were collected under the following condition: 780 nm laser source, 20X objective lens, 24 mW laser power, and 0.5 s exposure time. The collected

area was then analyzed with image analysis. For *in situ* method, Raman maps were collected with roughly 4,000,000  $\mu\text{m}^2$  area with 80  $\mu\text{m}$  image pixel size from a flour pellet. For extraction method, Raman maps were collected with 1,000,000 ~ 4,000,000  $\mu\text{m}^2$  area with 80  $\mu\text{m}$  image pixel size depending on the sample droplet's size. For BPO identification, a peak of 1780  $\text{cm}^{-1}$  was used. The BPO Raman maps were analyzed using the OMNIC software with image analysis. Image analysis tells the percentage of the target compound present within an area. This percentage can be used to make preliminary predictions for the sample's concentration. Image analysis also provided peaks assignment and intensity for target compound in the chosen area.

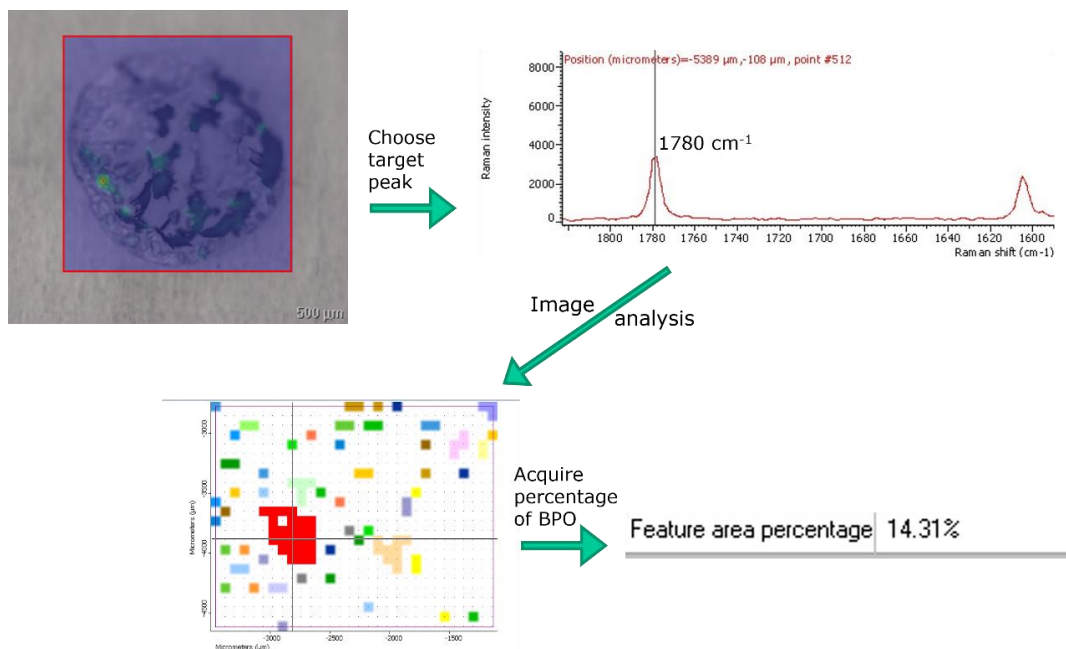


Figure 17: demonstrations of BPO Raman analysis. Peaks at 1780  $\text{cm}^{-1}$  are used to process image analysis and acquire BPO's area percentage.

### 3.3 Result and discussion

#### 3.3.1 *In situ* method

This *in situ* method is used to determine the lowest BPO concentration that can be tested without extracting from the flour. According to the table 1, 5% of BPO flour shows roughly 12% of BPO present within the tested area. One batch of 2% BPO flour is highlight as an outlier because 4~5% is the normal percentage for 2% BPO flour. The reason I was only getting 0.25% here was probably because the area I collect has little BPO(Table 1). This uneven distribution of BPO in the flour pellet might be due to the BPO not mixing well in the flour sample. The percentage can be used to predict a preliminary guess for the sample's concentration. However, the detection limit for this method is not low enough. For sample's concentration smaller than 0.1%, there is only around 0.5% area of BPO present. In other words, this *in situ* method cannot be used to detect as low as the BPO regulation, which is 75 ppm.

	Concentrations	5%	2%	1%	0.5%	0.1%
Image analysis	Batch 1	14.58%	0.25%	1.72%	4.60%	0.80%
percentage	Batch 2	11.60%	2.90%	3.33%	1.86%	0.15%

Table1: percentage of area showing BPO signal in chosen mapping from image analysis. Highlight percentage represent the outlier for 2% BPO flour.

### 3.3.2 Extraction method

A simple BPO extraction was done by adding organic solvent (acetonitrile) into BPO flour. The BPO dissolved in acetonitrile and was extracted with supernatant after the centrifugation. By using extraction method, 5% flour showed 40% of BPO signal area, and even 0.1% flour showed 15% of BPO (Table2). Extraction method showed a higher percentage of BPO presenting compared to the *in situ* method in table 1. However, lower concentrations, 0.05% and 0.01%, did not show any of BPO present (Figure 18A, 18B).

	Concentration	5%	1%	0.1%
Image analysis percentage	Batch 1	38.33%	26.52%	14.35%
	Batch 2	47.88%	27.33%	17.10%

Table 2: percentage of area showing BPO signal in chosen mapping by extraction method.

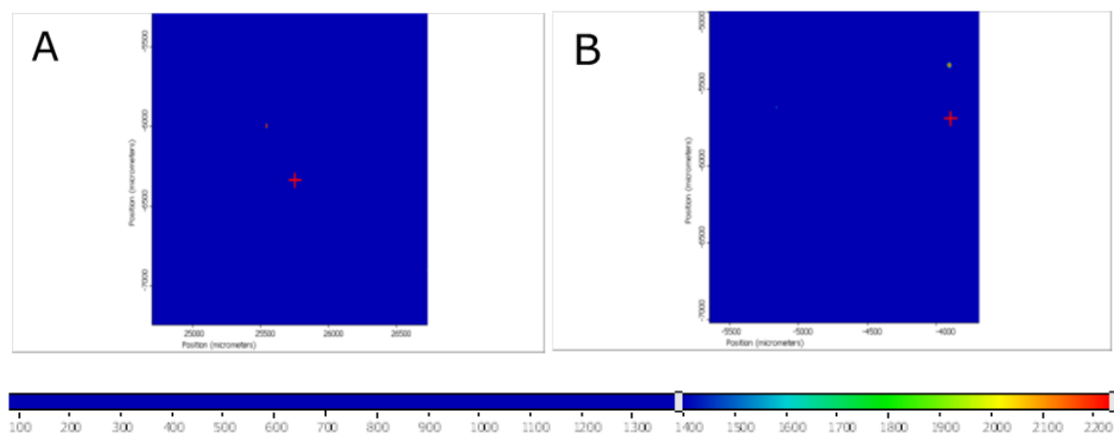


Figure 18: mapping images of BPO flour detected by Thermo Scientific DXRxi Spectro-microscope.

A: 0.05% BPO flour. B: 0.01% BPO flour

The extraction method was improved with evaporating step. BPO can be detected in low concentration, such as 0.05% and 0.01% flour. Figures 19 and 20 show three duplicates of sample droplets. Although the BPO signal can be determined in low concentration with this improved method, the issue is inconsistent results, in which not all replicates show BPO signal.

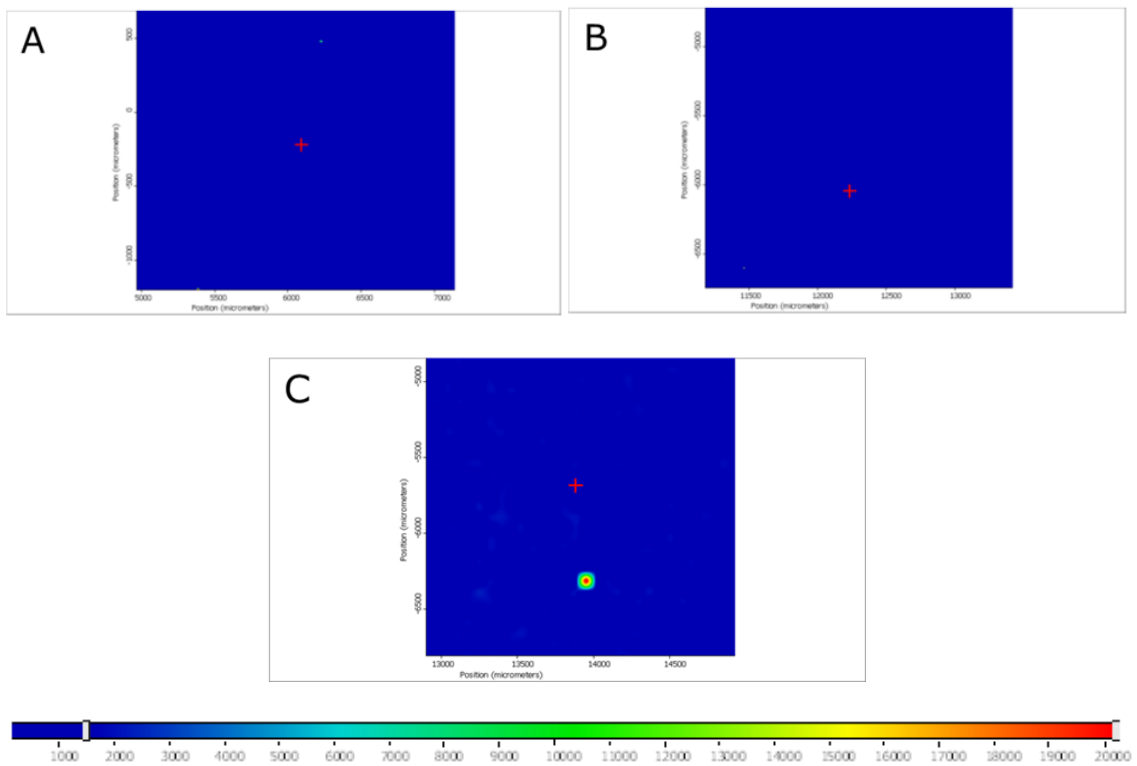


Figure 19: three replicates mapping images for 0.05% BPO flour detect by DXRxi Spectro-microscope.

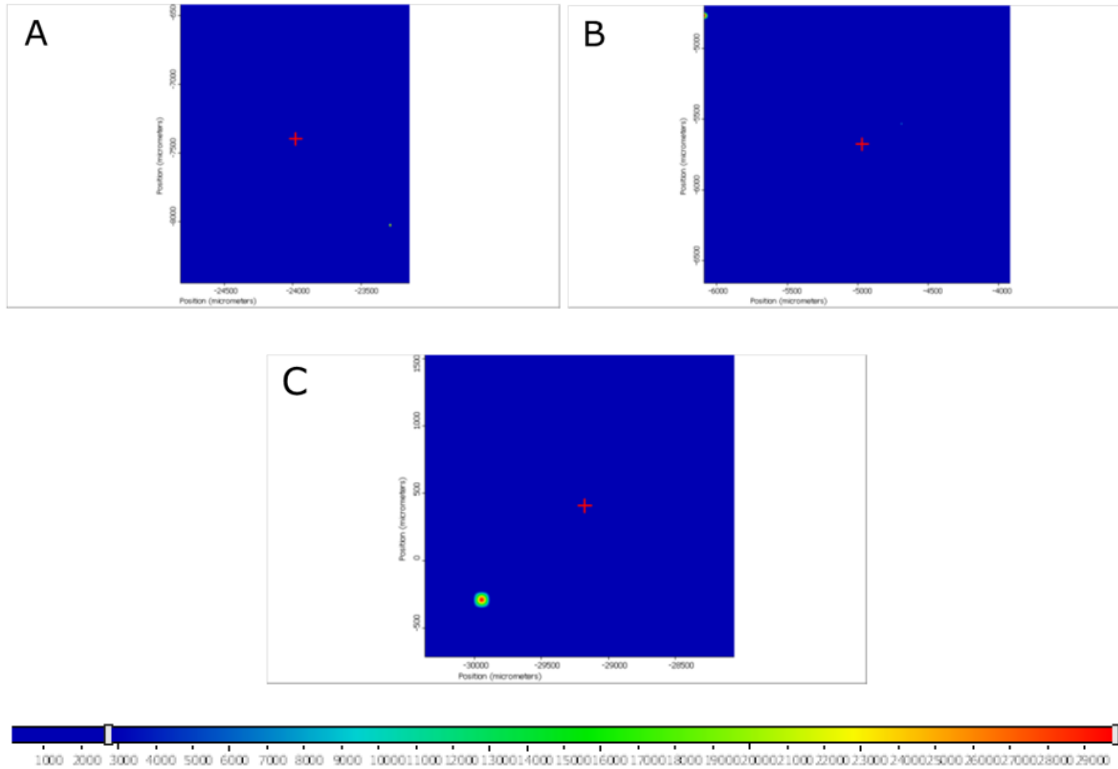


Figure 20: three replicates mapping images for 0.01% BPO flour detect by DXRxi Spectro-microscope.

To test out if BPO was lost during the evaporating step, we spiked the BPO in the sample after the evaporation step. Figure 21 shows the mapping image of BPO spiked after the evaporating steps. Both replicates show consistent BPO presenting. That said during the evaporating step, BPO did not escape as acetonitrile evaporate.

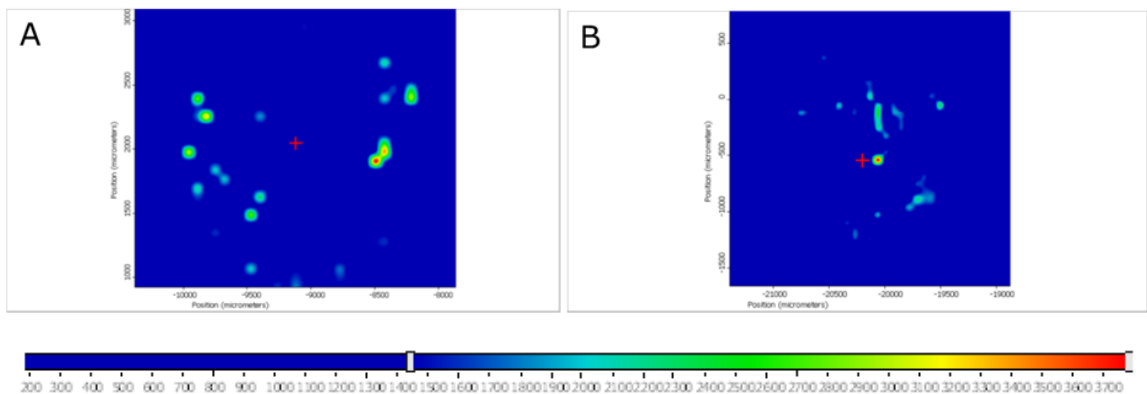


Figure 21: two replicate mapping images for 75 ppm spiking BPO samples detect by DXRxi Spectro-microscope

The extraction method with the evaporate step gave inconsistent BPO signals for low concentrations. However, spiking BPO procedure with evaporate step provided a consistent and observable result even in the low concentration, 75 ppm (Figure 21). The inconsistent result may be from the extraction method, as matrices in flour dissolved in acetonitrile along with BPO affected its signal. C18 SPE column was used to further improve the extraction method. With the assistance of C18 column, 0.1% BPO originally in flour provides roughly 25% area of BPO (Figure 22), which is enhanced than the previous extraction method (table 1, 2). Compared to 0.1% BPO spiking procedure (Figure 23), 0.1% BPO originally in flour with improved extraction method (evaporate step+C18 SPE column) resulted in a reasonable 62% of recovery percentage. Although BPO recovery percentage could be higher by using the HPLC, which ranged from 96.1% to 102.6% (35), the proposed method had the greatest advantage compared to the HPLC. This extraction method did not convert BPO into BA during sample preparation, which means we could qualify and quantify BPO amount from a sample containing both BPO and BA. In addition, the sample preparation and detection steps were straight-forward. Each mapping image sample took roughly 20 minutes to prepare and 9 minutes to detect by DXRxi microscope. Compared to the current method, HPLC required at least 30 minutes of sample preparation (37), and the detention time can be about 20-30 minutes depending on the flow rate. (50) In other words, the extraction method developed not only prevented BPO degradation, but also provided a more rapid detection for BPO in flour.

After all, the image analysis used in this chapter demonstrated the potential of a sensitive and reliable approach for BPO detection in flour. Future experiments are needed

to further improve the recovery, evaluate and validate the quantitative capability of Raman mapping for BPO detection in flour and other food matrices.

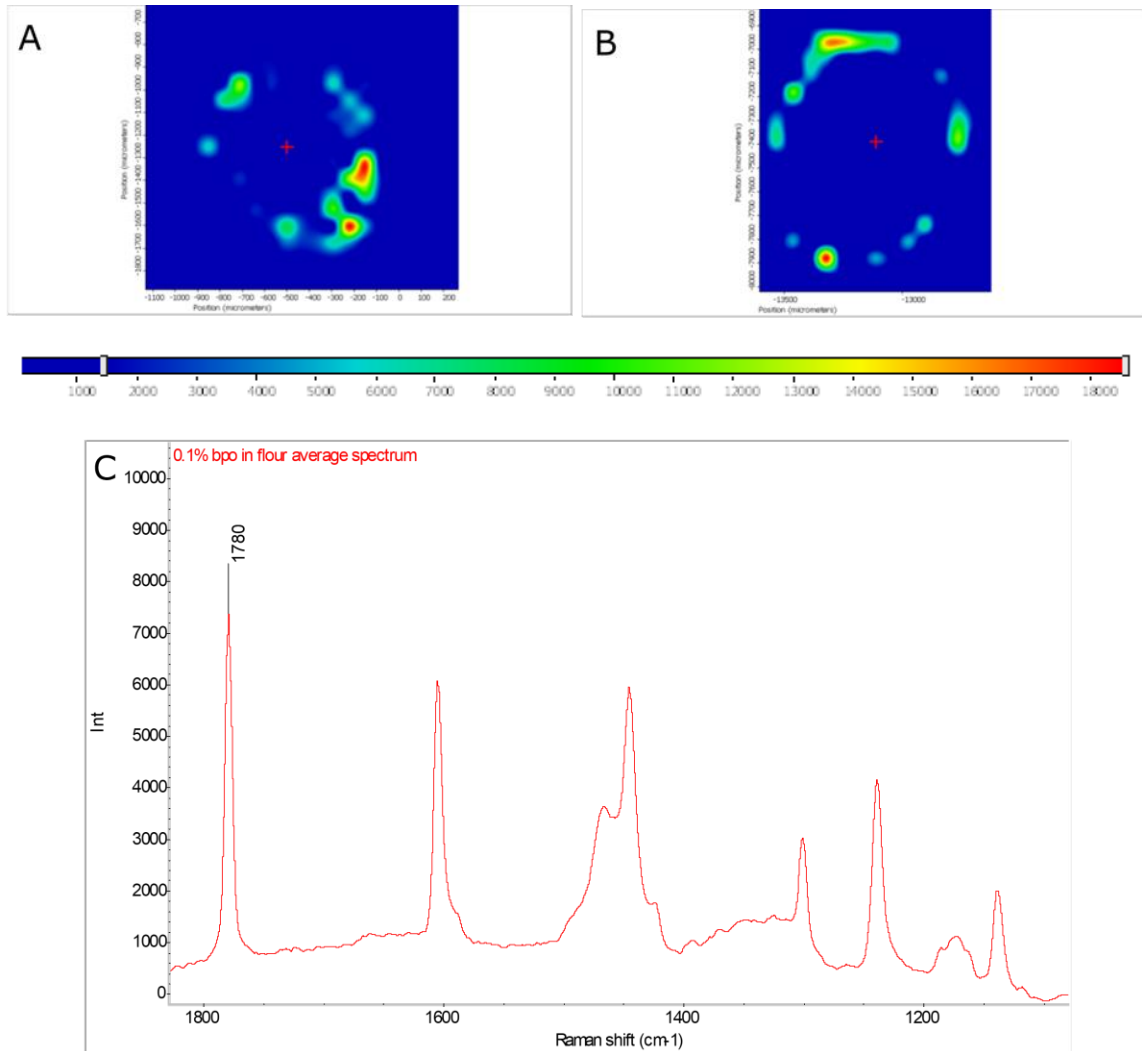


Figure 22: two replicate mapping images for 0.1% BPO originally in flour. A provides 28.96% area of BPO presenting, and B provides 22.73% area of BPO presenting according to image analysis. (C) represents the average spectrum (A) and (B)

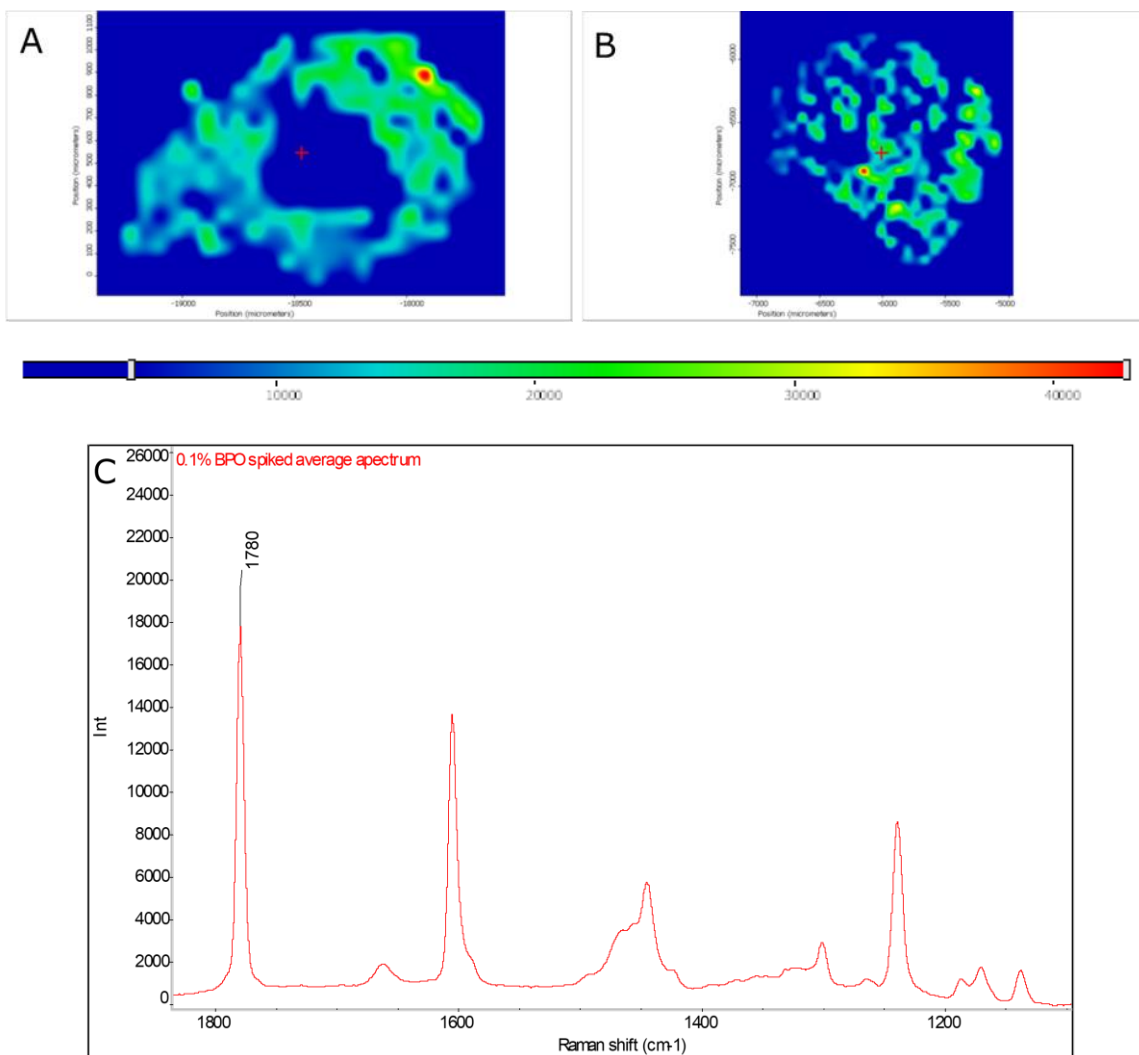


Figure 23: two replicate mapping images for 0.1% spiking BPO procedure. A shows 46.60% area of BPO presenting, and B shows 35.21% area of BPO presenting according to image analysis. (C) represents the average spectrum of (A) and (B)

### 3.4 Conclusion

In this study, we have developed a Raman-spectroscopy based method that can be used to quantify BPO in flour. *In situ* method without extracting, BPO can be used for preliminary tests, but it is not suitable for concentrations lower than 0.1%. A simple extraction method for BPO in flour improved the BPO signal in low concentrations but

not good enough for detecting the regulation concentration (i.e., 75 ppm). Although the extraction method with the evaporate step enhanced the lowest detection concentration, the BPO result was inconsistent at lower concentrations. Lastly, the extraction method was improved with the evaporate step and a C18 SPE spin column which yielded consistent mapping image data and a decent 62% recovery percentage. This Raman spectroscopic based extraction method has several advantages compared to HPLC. For instance, it is rapid, does not require skilled operators, and does not result in BPO conversion. Therefore, the established extraction method supports the reliable quantitative analysis of BPO in flour. Future experiments will focus on further improving the recovery to meet the HPLC's level and evaluate and validate the quantitative capability of Raman mapping for BPO detection in flour and other food matrices.

1. Huang, A. C., Huang, C. F., Xing, Z. X., Jiang, J. C., & Shu, C. M. (2019). Thermal hazard assessment of the thermal stability of acne cosmeceutical therapy using advanced calorimetry technology. *Process Safety and Environmental Protection*, 131, 197-204.
2. Tan, Y., Xu, Y., Shang, Y., Wang, H., Li, W., & Cao, W. (2020). Thermal Decomposition Behavior and Thermal Hazard of Benzoyl Peroxide under Different Environmental Conditions. *ChemistrySelect*, 5(17), 5049-5054.
3. Slaga, T. J., Klein-Szanto, A. J., Triplett, L. L., Yotti, L. P., & Trosko, K. E. (1981). Skin tumor-promoting activity of benzoyl peroxide, a widely used free radical-generating compound. *Science*, 213(4511), 1023-1025.
4. Warth, A. D. (1991). Mechanism of action of benzoic acid on *Zygosaccharomyces bailii*: effects on glycolytic metabolite levels, energy production, and intracellular pH. *Applied and environmental microbiology*, 57(12), 3410-3414.
5. El-Samragy, Y. (2004). Benzoyl peroxide chemical and technical assessment. In *Joint FAO/WHO Expert Committee on Food Additives, 61st meeting*.
6. How harmful is flour whitener? (2008, September). Retrieved from <http://jamespang.com/health/how-harmful-is-flour-whitener>
7. World Health Organization. (2000). Benzoic acid and sodium benzoate: concise International chemical assessment document, 26. *WHO: Geneva*.
8. Saiz, A. I., Manrique, G. D., & Fritz, R. (2001). Determination of benzoyl peroxide and benzoic acid levels by HPLC during wheat flour bleaching process. *Journal of agricultural and food chemistry*, 49(1), 98-102.
9. Ponghong, K., Supharoek, S. A., Siriangkhawut, W., & Grudpan, K. (2015). A rapid and sensitive spectrophotometric method for the determination of benzoyl peroxide in wheat flour samples. *journal of food and drug analysis*, 23(4), 652-659.
10. Wang, C., & Hu, X. (2005). Determination of benzoyl peroxide levels in wheat flour and pharmaceutical preparations by differential pulse voltammetry in nonaqueous media. *Analytical letters*, 38(13), 2175-2187.
11. Xu, X., Li, H., Hasan, D., Ruoff, R. S., Wang, A. X., & Fan, D. L. (2013). Near-field enhanced plasmonic-magnetic bifunctional nanotubes for single cell bioanalysis. *Advanced Functional Materials*, 23(35), 4332-4338.
12. Smith, E., & Dent, G. (2005). Modern Raman spectroscopy: a practical approach.
13. Haynes, C. L., McFarland, A. D., & Van Duyne, R. P. (2005). Surface-enhanced Raman spectroscopy.
14. Mikac, L., Ivanda, M., Gotić, M., Ristić, D., Đerek, V., Gebavi, H., ... & D'Andrea, C. (2015, May). Preparation and characterization of SERS substrates: From colloids to solid substrates. In *2015 38th International Convention on Information and Communication Technology, Electronics and Microelectronics (MIPRO)* (pp. 9-11). IEEE.
15. Murugesan, B., & Yang, J. (2019). Tunable Coffee Ring Formation on Polycarbonate Nanofiber Film for Sensitive SERS Detection of Phenylalanine in Urine. *ACS omega*, 4(12), 14928-14936.
16. Vickers, S., Bernier, M., Zambrzycki, S., Fernandez, F. M., Newton, P. N., & Caillet, C. (2018). Field detection devices for screening the quality of medicines: a systematic review. *BMJ global health*, 3(4).
17. Nie, X., Chen, Z., Tian, Y., Chen, S., Qu, L., & Fan, M. (2020). Rapid Detection of Trace Formaldehyde in Food Based on Surface-enhanced Raman Scattering Coupled with Assembled Purge Trap. *Food Chemistry*, 127930.
18. Zhu, J., Agyekum, A. A., Kutsanedzie, F. Y., Li, H., Chen, Q., Ouyang, Q., & Jiang, H. (2018). Qualitative and quantitative analysis of chlorpyrifos residues in tea by surface-enhanced Raman spectroscopy (SERS) combined with chemometric models. *LWT*, 97, 760-769.
19. Fu, X., Chen, J., Fu, F., & Wu, C. (2020). Discrimination of talcum powder and benzoyl peroxide in wheat flour by near-infrared hyperspectral imaging. *Biosystems Engineering*, 190, 120-130.
20. Yin, M., Zhang, C., Li, J., Li, H., Deng, Q., & Wang, S. (2019). Highly sensitive detection of benzoyl peroxide based on organoboron fluorescent conjugated polymers. *Polymers*, 11(10), 1655.
21. Rezaee, M., Assadi, Y., Hosseini, M. R. M., Aghaee, E., Ahmadi, F., & Berijani, S. (2006). Determination of organic compounds in water using dispersive liquid-liquid microextraction. *Journal of Chromatography A*, 1116(1-2), 1-9.
22. Ding, M., Liu, W., Peng, J., Liu, X., & Tang, Y. (2018). Simultaneous determination of seven preservatives in food by dispersive liquid-liquid microextraction coupled with gas chromatography-

- mass spectrometry. *Food chemistry*, 269, 187-192.
23. Singh, N., & Ahmad, A. (2014). Synthesis and spectrophotometric studies of charge transfer complexes of p-nitroaniline with benzoic acid in different polar solvents. *Journal of Molecular Structure*, 1074, 408-415.
  24. Aung, H. P., & Pyell, U. (2016). In-capillary derivatization with o-phthalaldehyde in the presence of 3-mercaptopropionic acid for the simultaneous determination of monosodium glutamate, benzoic acid, and sorbic acid in food samples via capillary electrophoresis with ultraviolet detection. *Journal of Chromatography A*, 1449, 156-165.
  25. Shan, D., Li, Q., Xue, H., & Cosnier, S. (2008). A highly reversible and sensitive tyrosinase inhibition-based amperometric biosensor for benzoic acid monitoring. *Sensors and Actuators B: Chemical*, 134(2), 1016-1021.
  26. Wang, J., Guo, X., & Jia, L. (2017). A simple method for the determination of benzoic acid based on room temperature phosphorescence of 1-bromopyrene/ $\gamma$ -cyclodextrin complex in water. *Talanta*, 162, 423-427.
  27. Jones, R. R., Hooper, D. C., Zhang, L., Wolverson, D., & Valev, V. K. (2019). Raman techniques: fundamentals and frontiers. *Nanoscale research letters*, 14(1), 1-34.
  28. Fan, M., Andrade, G. F., & Brolo, A. G. (2011). A review on the fabrication of substrates for surface enhanced Raman spectroscopy and their applications in analytical chemistry. *Analytica chimica acta*, 693(1-2), 7-25.
  29. Cho, I. H., Bhandari, P., Patel, P., & Irudayaraj, J. (2015). Membrane filter-assisted surface enhanced Raman spectroscopy for the rapid detection of E. coli O157: H7 in ground beef. *Biosensors and Bioelectronics*, 64, 171-176.
  30. Schlücker, S. (2014). Surface-Enhanced raman spectroscopy: Concepts and chemical applications. *Angewandte Chemie International Edition*, 53(19), 4756-4795.
  31. Li, Y., Peng, Y., Chao, K., Qin, J., & Dhakal, S. (2019, April). Nondestructive rapid detection of benzoyl peroxide in flour based on Raman hyperspectral technique. In *Sensing for Agriculture and Food Quality and Safety XI* (Vol. 11016, p. 110160G). International Society for Optics and Photonics.
  32. Bao, L. L., Mahurin, S. M., Liang, C. D., & Dai, S. (2003). Study of silver films over silica beads as a surface-enhanced Raman scattering (SERS) substrate for detection of benzoic acid. *Journal of Raman Spectroscopy*, 34(5), 394-398.
  33. Ponghong, K., Supharoek, S. A., Siringkhawut, W., & Grudpan, K. (2015). A rapid and sensitive spectrophotometric method for the determination of benzoyl peroxide in wheat flour samples. *Journal of food and drug analysis*, 23(4), 652-659.
  34. Wang, X., Huang, W., Zhao, C., Wang, Q., Liu, C., & Yang, G. (2017). Quantitative analysis of BPO additive in flour via Raman hyperspectral imaging technology. *European Food Research and Technology*, 243(12), 2265-2273.
  35. Mu, G., Liu, H., Gao, Y., & Luan, F. (2012). Determination of benzoyl peroxide, as benzoic acid, in wheat flour by capillary electrophoresis compared with HPLC. *Journal of the science of food and agriculture*, 92(4), 960-964.
  36. El-Samragy, Y. (2004). Benzoyl peroxide chemical and technical assessment. In *Joint FAO/WHO Expert Committee on Food Additives, 61st meeting*.
  37. Wang, Q., Shi, W., & Hou, C. (2010). Determination of benzoyl peroxide content in wheat products by high-performance liquid chromatography. *Journal of food processing and preservation*, 34(3), 414-424.
  38. Lopez-Lorente, A. I., Simonet, B. M., & Valcarcel, M. (2013). Qualitative detection and quantitative determination of single-walled carbon nanotubes in mixtures of carbon nanotubes with a portable Raman spectrometer. *Analyst*, 138(8), 2378-2385.
  39. Lee, K. M., Herrman, T. J., & Yun, U. (2014). Application of Raman spectroscopy for qualitative and quantitative analysis of aflatoxins in ground maize samples. *Journal of Cereal Science*, 59(1), 70-78.
  40. Rojas, L. M., Qu, Y., & He, L. (2021). A facile solvent extraction method facilitating surface-enhanced Raman spectroscopic detection of ochratoxin A in wine and wheat. *Talanta*, 224, 121792.
  41. Schlücker, S. (2014). Surface-Enhanced raman spectroscopy: Concepts and chemical applications. *Angewandte Chemie International Edition*, 53(19), 4756-4795.
  42. Cho, I. H., Bhandari, P., Patel, P., & Irudayaraj, J. (2015). Membrane filter-assisted surface enhanced Raman spectroscopy for the rapid detection of E. coli O157: H7 in ground beef. *Biosensors and Bioelectronics*, 64, 171-176.

43. Zhao, B., Yang, T., Qu, Y., Mills, A. J., Zhang, G., & He, L. (2020). Rapid capture and SERS detection of triclosan using a silver nanoparticle core–protein satellite substrate. *Science of The Total Environment*, 716, 137097.
44. Gukowsky, J. C., Xie, T., Gao, S., Qu, Y., & He, L. (2018). Rapid identification of artificial and natural food colorants with surface enhanced Raman spectroscopy. *Food Control*, 92, 267-275.
45. Li, Y., Peng, Y., Chao, K., Qin, J., & Dhakal, S. (2019, April). Nondestructive rapid detection of benzoyl peroxide in flour based on Raman hyperspectral technique. In *Sensing for Agriculture and Food Quality and Safety XI* (Vol. 11016, p. 110160G). International Society for Optics and Photonics.
46. Bao, L. L., Mahurin, S. M., Liang, C. D., & Dai, S. (2003). Study of silver films over silica beads as a surface-enhanced Raman scattering (SERS) substrate for detection of benzoic acid. *Journal of Raman Spectroscopy*, 34(5), 394-398.
47. Kang, L., Wang, K., Li, X., & Zou, B. (2016). High pressure structural investigation of benzoic acid: raman spectroscopy and x-ray diffraction. *The Journal of Physical Chemistry C*, 120(27), 14758-14766.
48. Wang, X., Huang, W., Zhao, C., Wang, Q., Liu, C., & Yang, G. (2017). Quantitative analysis of BPO additive in flour via Raman hyperspectral imaging technology. *European Food Research and Technology*, 243(12), 2265-2273.
49. Ji-wei, M. A. (2008). Determination on Benzoyl Peroxide in Wheat Flour by HPLC [J]. *Journal of Anhui Agricultural Sciences*, 21.
50. Abe-Onishi, Y., Yomota, C., Sugimoto, N., Kubota, H., & Tanamoto, K. (2004). Determination of benzoyl peroxide and benzoic acid in wheat flour by high-performance liquid chromatography and its identification by high-performance liquid chromatography–mass spectrometry. *Journal of chromatography A*, 1040(2), 209-214. How harmful is flour whitener? (2008, September). Retrieved from <http://jamespang.com/health/how-harmful-is-flour-whitener>
51. Abe-Onishi, Y., Yomota, C., Sugimoto, N., Kubota, H., & Tanamoto, K. (2004). Determination of benzoyl peroxide and benzoic acid in wheat flour by high-performance liquid chromatography and its identification by high-performance liquid chromatography–mass spectrometry. *Journal of chromatography A*, 1040(2), 209-214.
52. Qin, J., Kim, M. S., Chao, K., Gonzalez, M., & Cho, B. K. (2017). Quantitative detection of benzoyl peroxide in wheat flour using line-scan macroscale Raman chemical imaging. *Applied spectroscopy*, 71(11), 2469-2476.
53. El-Samragy, Y. (2004). Benzoyl peroxide chemical and technical assessment. In *Joint FAO/WHO Expert Committee on Food Additives, 61st meeting*.
54. Ponghong, K., Supharoek, S. A., Siringkhawut, W., & Grudpan, K. (2015). A rapid and sensitive spectrophotometric method for the determination of benzoyl peroxide in wheat flour samples. *Journal of food and drug analysis*, 23(4), 652-659.